Variation and Environmental Association of Ecosystem Metabolism in the Lower Klamath River: 2007-2014

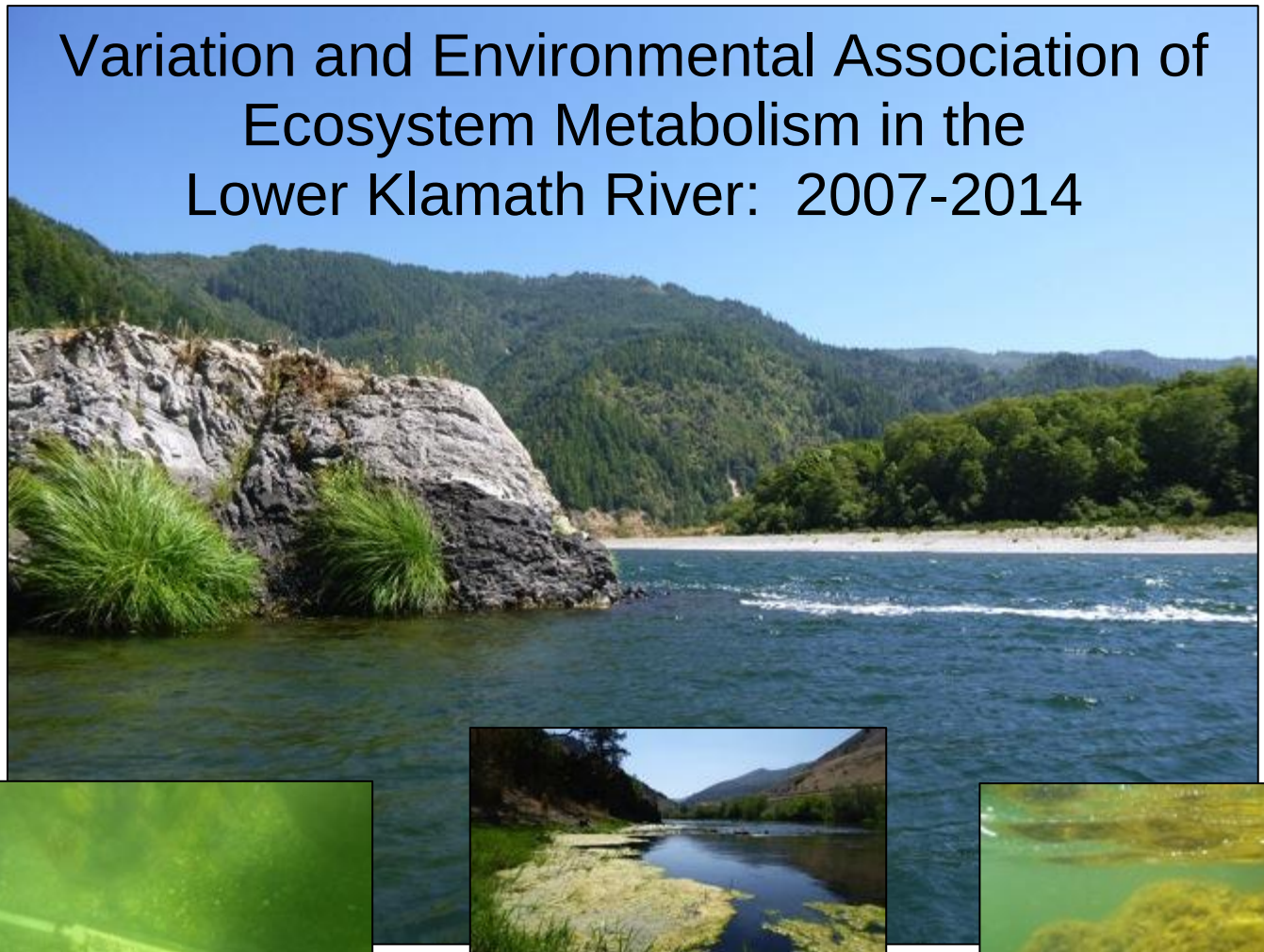

Laurel Genzoli
University of Wyoming

Robert O. Hall
University of Wyoming

J. Eli Asarian
Riverbend Sciences

Jacob Kann
Aquatic Ecosystem Sciences, LLC.

Prepared for:
Klamath Tribal Water Quality Consortium
December 2015

Variation and Environmental Association of Ecosystem Metabolism in the Lower Klamath River: 2007-2014

Laurel Genzoli and **Robert O. Hall**
University of Wyoming
Laramie, Wyoming

J. Eli Asarian
Riverbend Sciences
Weaverville, California

Jacob Kann
Aquatic Ecosystem Sciences, LLC.
Ashland, Oregon

Prepared for:
Klamath Tribal Water Quality Consortium
December 2015

Suggested citation:

Genzoli, L., R.O. Hall, J.E. Asarian, and J. Kann. 2015. Variation and Environmental Association of Ecosystem Metabolism in the Lower Klamath River: 2007-2014. Prepared by the University of Wyoming, Riverbend Sciences, and Aquatic Ecosystem Sciences LLC. for the Klamath Tribal Water Quality Consortium. 44p. + appendices.

EXECUTIVE SUMMARY

The Klamath River and some of its tributaries are designated on the Clean Water Act (CWA) Section 303(d) list as impaired water bodies. Water quality is a concern in the Klamath River because it affects culturally and economically important salmon fisheries as well as public health. During the summer months, photosynthesis by aquatic plants and algae attached to the streambed elevate dissolved oxygen (O_2) concentrations during the day, creating a 24-hour cycle in dissolved O_2 concentrations. Respiration at night by those same organisms and bacteria has the reverse effect, depressing dissolved O_2 levels. Resulting low nighttime dissolved O_2 concentrations can exceed water quality standards and be stressful to fish (NCRWQCB 2010).

Ecosystem metabolism describes the fixation of organic carbon (gross primary production, GPP) and the mineralization of organic carbon (ecosystem respiration, ER). GPP and ER are integrative measures of river ecosystem health, and are complementary to more commonly used structural metrics that are regularly monitored on the Klamath River, such as dissolved O_2 concentration, water temperature, and periphyton biomass. Ecosystem metabolism directly controls dissolved O_2 concentrations in aquatic ecosystems and algal biomass, in part, forms the base of animal productivity in river food-webs (Thorp and Delong 2002, Cross et al. 2013).

Time series of daily metabolism estimates across many years allows examination of controls on metabolism at multiple time scales. Knowing what drives metabolism in the Klamath River will allow us to predict how rates of GPP and ER, and in turn, dissolved O_2 concentrations will respond to changes in environmental conditions and management actions. Additionally, rates and patterns in ecosystem metabolism may be useful explanatory variables in other studies conducted in the Klamath River.

We calculated daily ecosystem metabolism from 2007 to 2014 from ~May–November at three sites (Seiad, Weitchpec, and Turwar) on the Lower Klamath River to quantify rates, patterns, and drivers of GPP and ER. We calculated GPP and ER using dissolved O_2 and water temperature data from water quality sondes maintained by the Karuk and Yurok tribes. We related rates of GPP to minimum dissolved O_2 to investigate how GPP controls levels of dissolved O_2 in the Klamath River. We investigated the effect of the reservoir-derived cyanobacterial bloom on GPP and ER by comparing metabolism rates before and during the cyanobacterial. We related summer means of GPP and ER to control variables, and we investigated controls on daily variation in GPP using multivariate time series models.

Rates of ecosystem metabolism varied through time and space on the Klamath River. Temporal variation occurred on multiple time scales including daily, seasonal, and annual. Rates of GPP and ER were generally low in the spring, peaked in the summer, and then decreased again in the fall. The six-month means of GPP and ER across all sites and years was 7.1 g O_2 m^{-2} d^{-1} and -5.9 g O_2 m^{-2} d^{-1}. Rates of GPP and ER generally decreasing at down-stream sites, such that Seiad had the highest mean GPP and ER at 9.2 and -6.9 g O_2 m^{-2} d^{-1}, mean GPP and ER at Weitchpec were 7.6 and -5.8 g O_2 m^{-2} d^{-1}, and mean GPP and ER at Turwar was 4.3 and -4.5 g O_2 m^{-2} d^{-1}.

Variation in daily GPP controlled variation in daily ER and daily minimum dissolved O_2 saturation. Variation in GPP explained 47%, 71%, and 73% of the variation in ER at Seiad, Weitchpec, and Turwar, respectively. Dissolved O_2 minima occurs at night when ER removes O_2 from the water without concurrent primary production, so high rates of GPP correlated with low daily dissolved O_2

minima, with dissolved O_2 predicted to sink below 90% saturation at ~13, ~15, and ~6 g O_2 m^{-2} d^{-1} at Seiad, Weitchpec, and Turwar respectively. During algal bloom conditions, the relationship between GPP and minimum daily dissolved O_2 values shifted such that dissolved O_2 minimum was expected to sink below 90% saturation at lower rates of GPP than during non-bloom conditions.

We focused the correlation analyses of intra- and inter- annual variation in metabolism on the summer months, which we defined as July, August, and September. Rates of GPP were low during high discharge, but rates of GPP spanned the full range of observed values during base-flow conditions, which occurred in summer months.

Mean summer metabolism metrics were related to summer base-flow rates in the Klamath River. Mean summer GPP and ER at Weitchpec and Turwar decreased as summer base-flow increased. At Seiad, net ecosystem production (NEP) was positively related to base-flow. Means of summer base-flow were highly correlated with other environmental variables that may influence rates of metabolism, making it difficult to determine which components of discharge (depth, width, velocity), or which covariates to discharge, were responsible for controlling the variability in summer metabolism. Means of summer water temperature, depth, total phosphorus, and total nitrogen were all highly correlated with mean discharge (> 64%, Pearson's correlation coefficient).

Multivariate time series models predicted daily variation in GPP in the Klamath River. We predicted measured rates of GPP using modeled light, the fraction of discharge originating from Iron Gate Dam, and the cyanobacterial bloom status of the river. The effect of the bloom was large at Seiad, where the model predicted GPP to decrease ~3.5 g O_2 m^{-2} d^{-1} from non-bloom to bloom conditions. The effect was smaller at down stream sites, with no bloom effect on total GPP at Turwar. These results supported the results of paired t-tests of GPP during non-bloom and bloom conditions across years. Increases in the fraction of discharge from Iron Gate from lowest observed summer levels to highest observed summer levels predicted an increase in GPP of ~3.5, ~9, and ~2 g O_2 m^{-2} d^{-1} at Seiad, Weitchpec, and Turwar respectively. GPP was predicted to increase with increasing light at all sites, with the biggest effect at Weitchpec, where steep canyon walls may amplify the effects of decreased day length.

Ecosystem metabolism on the Klamath River was variable at multiple time scales, allowing us to assess that variation both among and within years. In both cases, discharge metrics were a predictor of metabolism. At higher flows, decreased metabolism is likely due to a combination of benthic scour, and reduced light associated with increased depth and decreased water clarity. During summer months, the focal period of this study, discharge generally decreased or remained stable. In these months, the effect of discharge on rates of metabolism may be due to some benthic light reduction due to increased depth, or changes in nutrient concentrations, which increased with an increased fraction of flow from Iron Gate. GPP was highly auto-correlated through time, and the limiting control on GPP changed through time, making the use of multivariate time series models useful in teasing apart the drivers of variation in daily rates of GPP. Understanding the specific mechanisms limiting production at the ecosystem level may require additional data collection including ambient light conditions representative of the light at the river surface, measurements of water clarity, and high frequency measurements of nutrient concentrations.

TABLE OF CONTENTS

* The electronic appendix is embedded as an attachment in the Portable Document Format (PDF) version of this report. To access the attachments, open the report in Adobe Acrobat and then click the paper clip icon to open the Attachments panel.

LIST OF FIGURES

LIST OF TABLES

1 INTRODUCTION

1.1 DESCRIPTION OF STUDY AREA

The Klamath River is one of the major salmon spawning and rearing rivers of the Western United States. Its uppermost tributaries originate in Southern Oregon and drain into Upper Klamath Lake, the Link River and Lake Ewauna, where the Klamath River begins. From this point, the river flows through a series of hydroelectric impoundments, including J.C. Boyle, Copco (I & II), and Iron Gate Reservoirs. Below Iron Gate Dam, the river flows 306 kilometers to the Pacific Ocean, mostly through a confined, bedrock canyon. The climate is Mediterranean, with cool, wet winters featuring rainfall at lower elevations and snow at higher elevations, and hot, dry summers that are moderated in downstream reaches by a cooling maritime influence. High winter and spring discharges, exceeding 3000 m^3/s every one to two years, are derived from heavy rain and snowmelt floods from tributaries below Iron Gate Dam. Summer and early autumn flows are low (hereafter referred to as base-flow) and these flows are primarily from Iron Gate Dam, with additional flows coming from the regulated Trinity River.

This study focused on the Lower Klamath River (i.e., downstream of Iron Gate Dam, Figure 1). The three study reaches spanned ~200 river km, over a range of geomorphic conditions and forest types. The most up-river site, Seiad, is in a constricted valley surrounded by dry mixed pine forest. The second site, Weitchpec, is characterized by steep canyon topography with mixed conifer forest. The river is confined within the canyon with well-defined rapids separated by pools. The final site, Turwar, is located nine kilometers upstream from the river's mouth, above the Klamath River Estuary. Summer base-flows at Turwar are approximately double those of upstream sites due to tributary inputs from the Trinity River. Vegetation and weather at Turwar is coastally influenced, with wetter, cooler conditions and more cloud cover. The primary source of nutrients to the Lower Klamath River is from the upper basin, and nutrient concentrations generally decrease in a downstream direction (Oliver et al. 2014).

1.2 BACKGROUND

The Klamath River and some of its tributaries are designated on the Clean Water Act (CWA) Section 303(d) list as impaired water bodies. The list of impairments varies by state and river reaches within states, but includes pH (only in Oregon reservoirs), water temperature, nutrients, organic enrichment/low dissolved O_2, sedimentation/siltation, ammonia toxicity, microcystin, and chlorophyll-a (NCRWQCB 2010). Total Maximum Daily Loads (TMDLs) have been developed for the river and its tributaries by the U.S. EPA, Oregon Department of Environmental Quality (ODEQ 2010) and the North Coast Regional Water Quality Control Board (NCRWQCB 2010). Water quality is a concern in the Klamath River because it affects culturally and economically important salmon fisheries as well as public health. During the warm summer months, dissolved O_2 follows a 24-hour cycle in which photosynthesis by aquatic plants and algae attached to the streambed (periphyton) elevate dissolved oxygen concentrations during the day. Respiration at night by those same organisms has the reverse effect, depressing dissolved O_2 levels (Nimick et al. 2011). The resulting low nighttime dissolved O_2 can exceed water quality standards and be stressful to fish (NCRWQCB 2010).

Functional indicators of river condition, which describe ecological processes, are an emerging means to assess river ecosystem health (Fellows et al. 2006, Young et al. 2008, Woodward et al. 2012). These metrics represent a mechanism to link anthropogenic alteration to ecosystem process and are complementary to more commonly used structural metrics that are regularly monitored on the Klamath River, such as dissolved O_2 concentration, water temperature, and periphyton biomass.

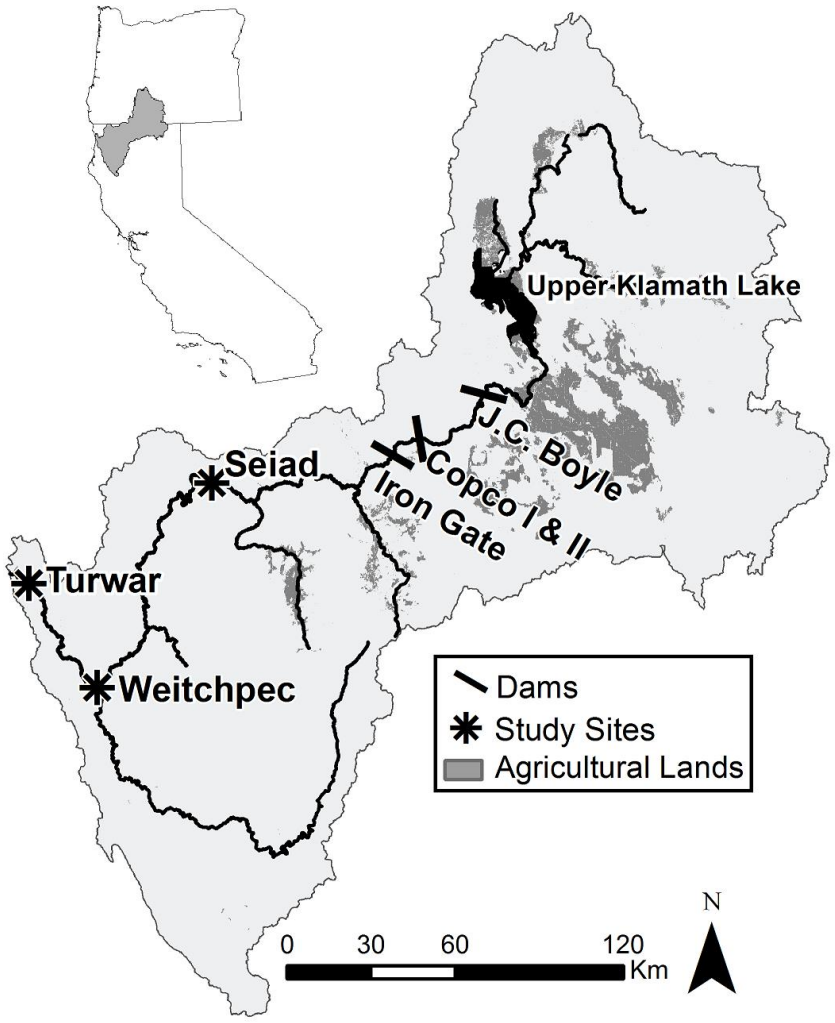

Figure 1. Location of sondes used for river metabolism calculations on the lower Klamath River.

Gross primary production (GPP) and ecosystem respiration (ER), collectively referred to as ecosystem metabolism, describe the fixation (via primary production) and mineralization (via respiration) of organic carbon in aquatic ecosystems. Ecosystem metabolism directly controls dissolved oxygen concentrations in aquatic ecosystems and algal biomass, and in part, forms the base of animal productivity in river food webs (Thorp and Delong 2002, Cross et al. 2013).

Net ecosystem production (NEP), which describes the balance of GPP and ER, can indicate the relative importance of terrestrial inputs versus in-stream primary production to a river. River and

stream research suggests that negative NEP (i.e., heterotrophy) is the common condition in flowing water, due to large subsides of terrestrial organic carbon (OC) from the surrounding watershed, productive upstream ecosystems, and light limitation to primary producers (Dodds 2006, Marcarelli et al. 2011). Autotrophy (i.e., positive NEP) may occur in rivers and streams that have limited terrestrial inputs relative to GPP, for example, where dams cut off the transport of OC and sediment from upstream, creating conditions for autotrophy in the resulting tailwater reach (Davis et al. 2012).

Continuous monitoring of ecosystem metabolism has shown that rates of GPP and ER can be as variable within a stream as those among biomes (Roberts et al. 2007). This variability within streams can be used to identify processes controlling metabolism within a single watershed, while considering that some controls on metabolism may have prolonged effects not generally taken into account in short duration studies (Uehlinger 2000, Beaulieu et al. 2013). Additionally, high frequency metabolism measurements are needed to accurately calculate seasonal metabolism estimates and variability in daily rates may in themselves be important indicators of ecosystem health (Roberts et al 2007, Palmer and Febria 2012). Long-term, high frequency dissolved O_2 data exists at multiple sites on the Lower Klamath River as part of water quality monitoring efforts, allowing the calculation of daily ecosystem metabolism during the spring, summer and fall.

Time series of daily metabolism estimates across many years allows examination of controls on metabolism at multiple time scales. Knowing what drives metabolism in the Klamath River will allow us to predict how rates of GPP and ER, and in turn, dissolved O_2 concentrations will respond to changes in environmental conditions and management actions. Additional research opportunities exist to relate river metabolism to pH, periphyton and macrophyte biomass, nutrients loads, and effects on the food web. As an integrative measure of river ecosystem condition, rates of river metabolism may be a useful metric for monitoring water quality and overall ecosystem health.

1.3 STUDY GOALS

While previous research evaluated Klamath River ecosystem metabolism during a single year (2012; Genzoli and Hall in revision), the overall goal of this study was to gain a multi-year understanding of ecosystem metabolism dynamics. Specifically, the goal was to assess inter-annual controls on metabolism and water quality on the Lower Klamath River. Specific objectives included: 1) calculation of daily rates of GPP and ER at three study sites during an eight-year period (2007-2014) during May–October when sondes were deployed in the river; 2) examine daily, seasonal, and longitudinal trends in GPP and ER to assess variability in river metabolism; 3) relate rates of river metabolism to daily minimum dissolved O_2 saturation; 4) relate variation in ER and GPP to environmental variables including the reservoir-born cyanobacteria blooms, river discharge, and light to identify major drivers of river metabolism on inter- and intra-annual scales.

2 METHODS

2.1 SITE SELECTION AND SONDE MEASUREMENTS

We selected three study reaches between Iron Gate Dam and the mouth of the Klamath River (Figure 1, Table 1). Reaches were immediately upstream of long-term water quality monitoring stations maintained by the Karuk Tribe Department of Natural Resources (Karuk DNR) and the Yurok Tribe Environmental Program (YTEP). Although additional water quality monitoring sites are maintained along the Klamath River (Asarian and Kann 2013), we only selected reaches where ecosystem metabolism could be calculated using the one-station method, based on criteria necessary for one-station estimates of metabolism (Chapra and DiToro 1991, M. Grace and R. Hall, unpublished data). This criterion requires that reaches have relatively uniform upstream physical characteristics including no major tributaries entering the reach for a distance of $1.6v/K$, which corresponds to turnover of 80% of dissolved O_2 in a river reach (where v is mean reach velocity (m/min) and K is the air-water gas exchange rate (1/min); Chapra and DiToro 1991). Additionally, we selected reaches where we could estimate atmospheric gas exchange using the night-time regression technique (Hornberger and Kelly 1974), which was not possible in reaches containing numerous large rapids that cause high rates of gas exchange (Hall et al. 2012).

Mulitparameter YSI sondes were deployed by YTEP and Karuk DNR at the three metabolism study sites annually from approximately May through October on the Klamath River (with some sites extending this season during some years). Sondes deployment was limited to an approximately six-month period due to budget and logistical constraints. Huge winter floods outside of this period make sondes inaccessible for maintenance and cause a risk of equipment loss. Additionally, sondes deployment was prioritized in the summer and fall when water quality impairment is common. Sondes measured and logged data (dissolved O_2 concentration, dissolved O_2 as percent saturation, water temperature, pH, specific conductivity, and florescence associated with blue-green algae pigments) every 30 min, and sondes were re-calibrated once every two weeks. During these years, sondes at Turwar and Weitchpec were maintained by YTEP and the sonde at Seiad was maintained by the Karuk DNR. Complete data collection methods and protocols are in water quality summary reports (Karuk Tribe 2008, 2010, 2011, 2012; Yurok Tribe 2010, 2011, 2012, 2013).

To provide consistency in dissolved O_2 measurements among years, we began calculating and analyzing metabolism data in 2007, the year that all[1] long-term mainstem monitoring sondes were upgraded to YSI 6600 EDS/V2 with optical dissolved O_2 sensors. Additionally, sondes at the three metabolism sites were equipped with phycocyanin sensors in 2007.

We used sonde data compiled by YTEP and the Karuk DNR for metabolism calculations, but made some revisions to the data in order to include as many days as possible in the daily metabolism dataset presented in this report. The metabolism model does not operate with missing O_2 or water temperature data. When three or fewer lines of data were missing (e.g., the

[1] Yurok Tribe also used optical probes in 2005 and 2006, but we did not include those years in our analysis because the Karuk Tribe's data at Seiad were collected using Hydrolab 4a probes which utilized the fouling-prone Clark's membrane method for dissolved O_2.

data lines were present with a time stamp, but data cells were populated with NAs) we interpolated the water temperature and dissolved O_2 data using nearby measurements. When no rows were present for missing data (e.g., the data jumped from 10:30 to 12:00), we did not attempt to add rows and interpolate data and we did not calculate metabolism for those days.

Calculations of ecosystem metabolism are sensitive to calibration errors. In two cases, we found calibration errors in the sonde measurements that we were able to correct. In 2011, days 159 to 171 at Seiad were calibrated high, as made apparent by a jump in minimum dissolved O_2 concentrations for a two-week period between re-calibrations. To correct this, we took the means of the minimum dissolved O_2 concentrations for two weeks before and after this period and subtracted it from the mean of the minimum dissolved O_2 level for the mis-calibrated period. We then subtracted the difference in those means from all of the O_2 data during the mis-calibrated period. At Turwar in 2014, there was a mis-calibration in the time stamp that caused the model to be skewed from the data for a two week period. We subtracted three hours from the time stamp from day 141 to day 154 to address this problem.

In other cases of sonde mis-calibration we excluded ER and NEP data from the analysis because ER estimates are sensitive to calibration errors. We excluded data from days 121 to 133 at Seiad in 2010 due to apparent low calibration during the first two weeks of the monitoring season. We did not attempt to correct the data because we didn't have data from prior to the calibration error. We excluded ER and NEP values at Weitchpec for all of 2007 because there were obvious shifts in dissolved O_2 highs and lows every two to four weeks that corresponded with sonde maintenance times.

Table 1. Site characteristics of metabolism study reaches on the Klamath River.

	Seiad	**Weitchpec**	**Turwar**
Site Code	SV	WE	KAT
Sonde Location (river km from mouth)	207	70	9
Elevation (m)	413	59	7
Barometric Pressure (mmHg)	725	755	760
Nearest USGS Gage	11520500	11523000	11530500
Reach Length (km)	7.6	6	40.7
Watershed Area (km^2)	27,600	32,200	40,600
Mean Depth (m)**	1.3	1.7	1.9
Mean Width (m) **	52	51	85
Mean Velocity (m/s)**	0.49	0.51	0.50
Discharge (m^3/s)*	106 (2847)	58 (1426)	36 (267)
Mean Total Nitrogen (mg/L)***	0.62	0.34	0.24
Mean Total Phosphorus (mg/L)***	0.14	0.07	0.04

* Discharge is mean of daily summer discharge (Jul, Aug, and Sep) followed by the mean of the largest flood for each water year during the study period.

** Mean reach depth and width were measured during base-flow conditions in 2012, and mean reach velocity was calculated based on these measurements and USGS discharge measurements.

*** Refers to the mean of the variable during summer months (Jul, Aug, and Sep).

2.2 AIR-WATER GAS EXCHANGE

We calculated air-water gas exchange from the high frequency dissolved O_2 data using the night-time regression method (Hornberger and Kelly 1974). At night when no light is available to support photosynthesis, the change in O_2 with time is:

$$\frac{\Delta O_2}{\Delta t} = ER + K(O_{2sat} - O_2) \quad (1)$$

where K (1/d) is the air-water gas exchange rate and $O_{2sat} - O_2$ is the dissolved O_2 deficit. We calculated K nightly at each site from May through October for 2010, 2011, and 2012 as the slope of the line produced in the regression from equation 1. We converted each K measurement to K_{600} (1/d) based on Schmidt number scaling to standardize K values across variable water temperatures (Jähne and Haußecker 1998). We calculated confidence intervals based on the regression slope for each K_{600} measurement and eliminated the 10% of measurements with the widest confidence intervals, resulting in 451, 455, and 445 K_{600} measurements at Seiad, Weitchpec, and Turwar, respectively. We plotted retained daily K_{600} values by daily discharge. We added a smoothing spline to our plots using the *smooth.spline* function in R (R Core Team 2013) with 10 degrees of freedom. We predicted K_{600} values daily at each site using daily mean discharge values with the site-specific gas exchange rate-discharge relationships (Figure 2).

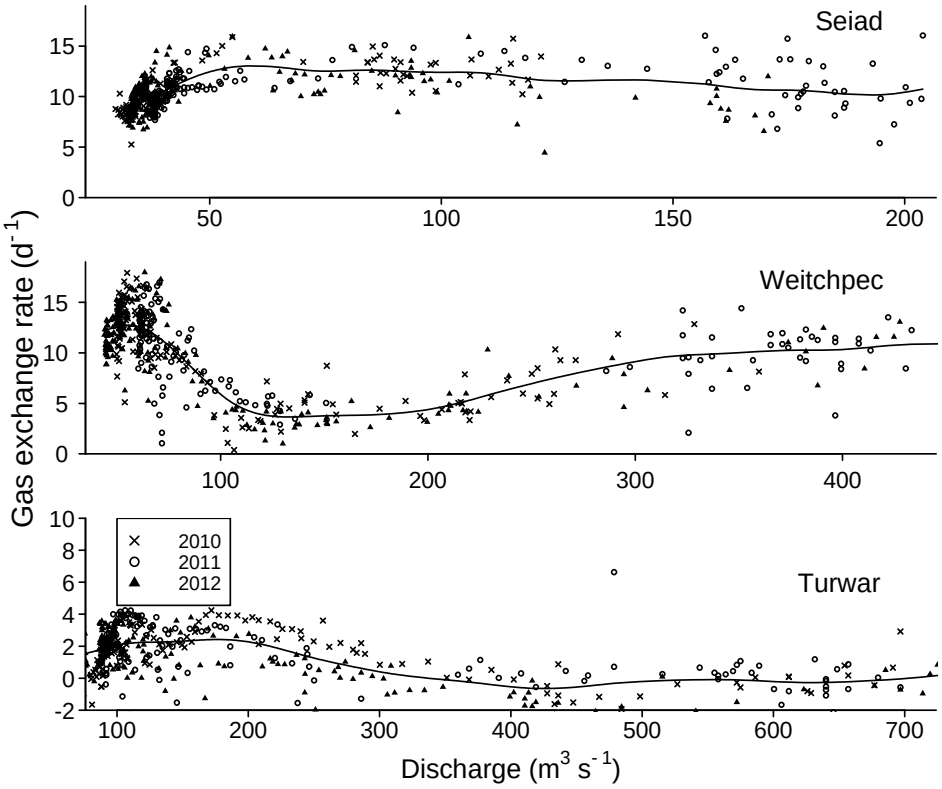

Figure 2. Daily gas exchange rate was non-linearly related to discharge at the three metabolism study reaches. Line is smooth spline fit of daily gas exchange rates from 2010 to 2012.

2.3 REACH-SCALE METABOLISM

We estimated reach-scale metabolism based on fitting O_2 data to a metabolism model (Van de Bogert et al. 2007):

$$mO_{2(t)} = mO_{2(t-1)} + \left(\frac{GPP}{\overline{z}} \times \frac{PPFD_{(t)}}{\sum PPFD_{24}} \right) + \left(\frac{ER}{\overline{z}} \times \Delta t \right) + K_{(t)}(O_{2sat(t)} - mO_{2(t-1)})\Delta t \qquad (2)$$

where mO_2 is modeled O_2 (mg/L) at time step t, GPP is g O_2 m^{-2} d^{-1}, $\overline{z}$ (m) is mean reach depth, $PPFD$ is solar insolation (µmol photons m^{-2} s^{-1}), $\sum PPFD_{24}$ is daily solar insolation (Yard et al. 2005), ER is g O_2 m^{-2} d^{-1}, Δt is the time between O_2 measurements (30 minutes in this study), and $K_{(t)}$ is K_{600} corrected for temperature at each time step. We used an extended day length to model metabolism that extended from 22:00 the previous night to 06:00 the morning following the day being calculated. To solve for GPP and ER, we fit equation 2 to the O_2 data, selecting the parameter values that minimized the negative log likelihood function of a normal distribution, using function *nlm* in R (R Core Team 2013, see appendix C for examples of model fits). We automated the computational process via a looping algorithm to estimate daily GPP and ER at each site. We calculated GPP for 1220, 1238, and 1255 days at Seiad, Weitchpec, and Turwar, respectively (Figure 2).

We calculated ER for the same days as GPP, except for days in which the minimum daily dissolved O_2 saturation never fell below 100% saturation. Supersaturation, due to bubble-mediated gas exchange in rapids during high discharge, prevents accurately estimating ER by causing calculation of positive ER values (Hall et al. 2012, Hall et al. 2015a). Supersaturation occurred rarely at Seiad, most often at Weitchpec, and moderately at Turwar, resulting in 1208, 1042, and 1187 daily ER calculations at these sites, respectively. Some underestimation may be present in ER calculations when supersaturation occurs through most, but not all of the day, however this generally happens during periods of high discharge and not during the time of year when metabolism drives lower water quality.

As an indicator of trophic state of the Klamath River, we calculated NEP by adding GPP to ER (a negative number), and were thus only able to calculate NEP when both GPP and ER were present for that day.

Table 2. Number of ecosystem metabolism measurements by month and year at each site. Number in parenthesis indicates number of ER and NEP measurements when dissolved O_2 was consistently supersaturated and therefore could not be calculated.

Seiad

	Apr	May	Jun	Jul	Aug	Sep	Oct	Nov	Dec
2007	0	0	10	20	19	27	15	0	0
2008	0	0	21	31	5	30	31	6	0
2009	0	14 (10)	27	14	25	3	18	0	0
2010	0	29 (17)	13	17	31	28	30	0	0
2011	2 (0)	23 (16)	29 (28)	31	31	30	31	3	0
2012	0	28	30	31	29	30	29	0	0
2013	5	31	28	29	31	30	31	1	0
2014	11 (9)	11	29	31	31	30	31	30	9

Weitchpec

	Apr	May	Jun	Jul	Aug	Sep	Oct	Nov	Dec
2007	0	9 (0)	28 (0)	31 (0)	29 (0)	28 (0)	8 (0)	0	0
2008	0	11 (0)	21 (9)	31	31	24	5	0	0
2009	0	10 (0)	28 (25)	31	31	30	31 (30)	2	0
2010	0	17 (0)	25 (5)	31	31	30	31 (27)	7 (4)	0
2011	0	14 (0)	26 (0)	19	31	30	31	4	0
2012	0	22 (0)	30 (24)	31	31	30	31	5	0
2013	0	16 (8)	30 (24)	30	23	30	9	0	0
2014	0	31 (19)	30	31	31	24	23	0	0

Turwar

	Apr	May	Jun	Jul	Aug	Sep	Oct	Nov	Dec
2007	0	10	26	30	31	30 (27)	6 (0)	0	0
2008	0	12	28	31	31	30	4	0	0
2009	0	12	30	31	31	30	8	0	0
2010	0	20 (6)	30 (20)	31	26	30	29 (27)	8 (7)	0
2011	0	8 (0)	30 (18)	23	31	30	31	5	0
2012	0	21 (9)	30	31	31	30	31	5	0
2013	0	18 (15)	30	31	31	30 (29)	14	0	0
2014	0	31	30	31	31	30	26 (25)	0	0

2.4 ENVIRONMENTAL DATA

2.4.1 CYANOBACTERIA BLOOM: TIMING AND MAGNITUDE

We calculated metrics to represent the timing and magnitude of the cyanobacteria bloom in the Klamath River, relying on data from real-time phycocyanin sensors, which record florescence in

the water and relate the florescence to calibrated blue-green algae concentrations. We calculated mean daily blue-green algal concentrations from the 30-minute interval sonde data, excluding the top and bottom 10% of the data to better represent the condition that most of the river is experiencing at during the day. We plotted daily means from all three sites for each year, and visually identified bloom periods (Appendix A). Not all years had continuous data at all three sites, and at times, among-site differences in patterns occurred. Because we expected the bloom to affect the river similarly with respect to relative concentration and timing (but not necessarily absolute algal concentration), we relied on two or more sites showing similar patterns in our identification of bloom timing).

2.4.2 DISCHARGE AND DEPTH

To enable calculations of river metabolism, we obtained daily stream discharge measurements from USGS gauging stations (Table 1). Gauging stations for Seiad and Turwar were located < 0.5 km from the sondes. The gauging station for Weitchpec was located 23 km up-river from the sonde. No major tributaries entered between gauging stations and sondes locations in any reach. To calculate mean depth for each day, we created rating curves for each site based on the relationship between mean depth and discharge (Holmquist-Johnson and Milhous 2010).

We included the daily mean discharge from Iron Gate Reservoir in the database (USGS gauging station number 11516530). We calculated the fraction of discharge originating from Iron Gate Reservoir daily at each site as the discharge released from Iron Gate Reservoir divided by the discharge at each metabolism study site.

2.4.3 SONDE DATA

We calculated water temperature metrics from the sonde data at each site, including mean water temperature over a 24-h period, minimum and maximum water temperatures during the day, and daily water temperature range as the difference between the maximum and minimum water temperature each day.

We calculated daily minimum dissolved O_2 saturation at each site from the dissolved O_2 concentration (mg/L) recorded by the sonde at each site using the equation from Garcia and Gordon (1992). We used temperature measurements from the sondes and the standard barometric pressure for the elevation of each sonde (Table 1). We then selected the minimum value of dissolved O_2 during each 24-h day.

2.4.4 LIGHT AND WEATHER DATA

We calculated daily-predicted light as the mean of the hourly *PPFD* (µmol photons m^{-2} s^{-1}) from light estimates used in the metabolism calculations above. These predictions were based on a light model that does not account for topographical features and does not take into account weather conditions or events such as smoke from fires (Yard et al. 2005), but captures seasonal patterns of light.

We obtained measured light (solar radiation in watts/m^2) from the Notchko Remote Automated Weather Station (Notchko RAWS). Although other RAWS stations exist (Oak Knoll, Somes Bar) along the lower Klamath River, data were most thorough over the eight-year study at the Notchko site. Solar radiation data from Notchko generally paralleled solar radiation data from

the next closest site, Somes Bar, but due to missing data and long periods of data that didn't match other sites, we elected to only use solar radiation data from Notchko. The Notchko RAWS site is located at ~river kilometer 48, and at 150 m elevation. We applied the Notchko solar radiation data to rates of metabolism at Weitchpec. Although the weather station is located about 22 kilometers below the bottom of the Weitchpec reach, it is likely more representative of conditions at Weitchpec due to its similar elevation and relative proximity. We did not include measured light data for Seiad or Turwar.

We included precipitation (daily totals measured in mm) in the metabolism database at each site. We used Oak Knoll RAWS for Seiad (located at river kilometer 253 and 591 m elevation), the the Somes Bar RAWS for Weitchpec (located at river kilometer 108, and 280 m elevation), and the Notchko RAWS for Turwar, based on site proximity.

2.4.5 NUTRIENT DATA

Nutrient samples were collected at a station near each of the three sonde sites ~every two weeks. Nutrient parameters included in this report include nitrate plus-nitrite (NO_3+NO_2, hear-on referred to as NO_3), total nitrogen (TN), soluble reactive phosphorus (SRP), and total phosphorus (TP). Nutrient concentrations are expressed in units of mg/L as N or mg/L as P. The Karuk and Yurok tribes collected and processed the nutrient with samples, with methodologies described in the following reports: Karuk Tribe (2007, 2008, 2010, 2011, 2012a, 2012b, 2013) and Yurok Tribe (2007, 2008, 2009, 2010b, 2011b, 2012b, 2013b).

We compared nutrient parameters to discharge metrics to assess the possibility of using flow rates as a daily proxy for nutrient concentration. We compared mean summer discharge rates with the mean of summer nutrient concentrations, and because the vast majority of nutrients in the Klamath River originate from upstream of Iron Gate Dam (Asarian and Kann 2010), we also compared nutrient samples (collected every two weeks) to the proportion of discharge originating from Iron Gate dam.

2.5 DATA ANALYSIS

2.5.1 RELATIONSHIPS BETWEEN GPP, ER, MINIMUM DAILY DISSOLVED O_2, AND CYANOBACTERIAL BLOOMS

To evaluate the hypothesis that cyanobacterial blooms would affect daily minimum dissolved O_2 concentrations, we used an analysis of covariance (ANCOVA) to test for a difference in the relationship between minimum daily dissolved O_2 saturation and daily GPP between periods with and without a cyanobacterial bloom. We first used an ANCOVA with an interaction term to tested for a differences in slopes of the relationships between GPP and minimum daily dissolved O_2 saturation at each site during bloom and non-bloom conditions. If there was no significant interaction term at a site, we used ANCOVA without an interaction term to test for the effect of the bloom (a difference in intercepts between bloom and non-bloom regressions). To determine what level of GPP correlates with minimum daily dissolved O_2 levels lower than the 90% saturation seasonal water quality goal during non-bloom conditions versus bloom

conditions, we performed simple linear regression at each site for bloom and non-bloom periods using all summer dates in the eight-year dataset.

2.5.2 INTER-ANNUAL CORRELATION ANALYSIS

To investigate annual patterns in ecosystem metabolism, we selected data from summer months (defined as July, August and September), when discharge is lowest and water quality problems peak on the Klamath River. We calculated summer means of daily metabolism data at Weitchpec and Turwar. At Seiad, we calculated means for each month, and then calculated the mean of the three months, in order to account for missing data from specific months in some years, which would otherwise skew the summer means (Table 2).

At each site, we calculated the summer means of environmental data including daily discharge (which we refer to as summer base-flow), the percent of discharge from Iron Gate Reservoir, water temperature, and nutrients. We included the magnitude and date of the largest flood during each water year (Oct. 1 the previous year to Sep. 30). We related these environmental variables to summer mean metabolism metrics.

We conducted simple linear regressions of the annual means of GPP, ER, and NEP with summer base-flow at each site. We compared environmental data to summer base-flows to identify covariates of base-flow.

2.5.3 DAILY TIME SERIES MODELS TO EVALUATE INTRA-ANNUAL CONTROLS ON GPP

To estimate short-term controls on variation of GPP in the Klamath River we developed linear regression models predicting GPP as a function of daily solar insolation, bloom status (coded as a dummy variable) and the fraction of Iron Gate flow. The latter we use as a proxy for nutrients because of the degree to which it covaries with SRP, though we recognize that other variables also vary with the fraction of Iron Gate flow such as mean depth and site-specific discharge. Like most time series, GPP is highly auto-correlated from day-to-day, and this autocorrelation needs to be accounted for in the model. We assumed an autoregressive process whereby GPP on one day is a function of GPP the day prior. We developed a Bayesian state-space time series model where the daily parameter estimate of GPP is known with observation (σ_{obs}) and process error (σ_{proc}) (Clark 2007).

$$GPP.obs_t = GPP_t + w_t \quad (3)$$

$$w_t \sim N(0, \sigma_{obs})$$

$$GPP_t = \theta \times GPP_{t-1} + \beta_0 + \beta_1 \times bloomstat + \beta_2 \times light + \beta_3 \times Q\ from\ IG + v_t \quad (4)$$

$$v_t \sim N(0, \sigma_{proc})$$

We solved for the parameters in a multi-level way by solving for each year with partial pooling of the βs among years (Gelman and Hill 2007). Pooling allows the parameters to differ among years, but the parameter estimates borrow strength from all years. Because this approach is Bayesian, we assigned minimally informative prior probabilities on the pooled βs. Prior for θ was uniform between 0 and 1 and represents the extremes between no correlation among days (θ = 0) to a random walk (θ = 1). We simulated the posterior distribution of the parameters using Markov-Chain Monte Carlo sampling using the program JAGS. The model parameters are in Appendix C.

Given the parameters β and θ, we want to know how much variation in these parameters controls variation in daily GPP. Because this model is an autoregressive time series, the mean value of GPP for any values of X is:

$$E(GPP) = \frac{\beta_0+\beta_1 X_1+\beta_2 X_2+\beta_3 X_3}{1-\theta} \quad (5)$$

We then calculated the estimated GPP (*E(GPP)*) at each site as a function of 5th and 95th quantiles of the fraction of flow from Iron Gate, algal bloom status, and light (modeled PPFD or measured solar radiation) to estimate the relative effect of variation in each of the predictors on GPP.

3 RESULTS

3.1 LONGITUDINAL AND TEMPORAL TRENDS IN DAILY METABOLISM RATES

Rates of ecosystem metabolism varied through time and space on the Klamath River. Temporal variation was evident on multiple time scales including daily, seasonal, and annual scales. Rates of GPP and ER changed daily, with a mean change of < 1 g O_2 m^{-2} d^{-1}, and never more than an increase or decrease of 8 g O_2 m^{-2} d^{-1} (Figure 3). Seasonally, rates of GPP and ER were lower in the spring (mean GPP and ER for May at all sites = 4.5 and -3.5 g O_2 m^{-2} d^{-1}), peaked in the summer (mean GPP and ER for August at all sites = 9.6 and -7.7 g O_2 m^{-2} d^{-1}), and then decreased again in the fall (mean GPP and ER for October at all sites = 4.7 and -3.5 g O_2 m^{-2} d^{-1}). Variation to the seasonal pattern is present, with some sites and years displaying high rates of GPP during the spring. Annually, GPP was higher during 2007-2009 (six-month mean = 8.2 g O_2 m^{-2} d^{-1}) than for the five more recent years (six-month mean = 6.6 g O_2 m^{-2} d^{-1}). Ecosystem respiration mirrored the rates and patterns of GPP, resulting in annual NEP medians and ranges that did not fluctuate much among years (Figure 4).

Longitudinal variation occurred in metabolism metrics. Rates of GPP and ER generally decreased from upstream to downstream sites. Mean six-month GPP was 9.5, 7.7, and 4.3 g O_2

m^{-2} d^{-1} at Seiad, Weitchpec and Turwar respectively. Mean six-month ER was -7.1, -5.9, and -4.7 g O_2 m^{-2} d^{-1} at Seiad, Weitchpec and Turwar respectively. The differences between rates of GPP and ER decreased from upstream to downstream sites, resulting in the lowest rates of NEP at Turwar (Figure 5). For all three metabolism metrics Turwar had a lower range than the upper two sites due to lower maximum rates of GPP and ER.

High rates of metabolism occurred on the Klamath River at both Seiad and Weitchpec. The 95th quantiles for GPP and ER at Seiad were 16.1 and -13.6 g O_2 m^{-2} d^{-1} and at Weitchpec were 14.7 and -12.1 g O_2 m^{-2} d^{-1}, respectively for May to October. More moderate rates of GPP and ER occurred at Turwar where the 95th quantiles for GPP and ER were 7.2 and -7.2 g O_2 m^{-2} d^{-1}.

Longitudinal patterns in GPP, ER, and NEP differed from year to year. From 2007 to 2012, GPP decreased from upstream to downstream sites (Figure 6). In 2013 and 2014, GPP at Seiad was lower than GPP at Weitchpec, while the median and range of GPP at Turwar remained the lowest. From 2007 to 2009, patterns in ER mirrored the patterns in GPP, with ER decreasing in a downstream direction. This pattern began to dissolve in 2010 when two or more sites displayed medians that were more similar in all remaining years. In 2011 and 2012, medians for ER were similar at all three sites. Net ecosystem productivity was lowest at Turwar in all years. In 2011 and 2012, there was a strong longitudinal pattern of decreasing NEP from upstream to downstream. In other years, NEP was similar to, or slightly lower than NEP at Weitchpec.

The three metabolism study reaches showed distinct seasonal patterns (Figure 7). A Locally Estimated Scatterplot Smoothing (LOESS) regression curve (Helsel and Hirsch 2002) fit to the daily GPP data at each site, using data from all years, shows that Turwar almost always had the lowest rates of GPP and lowest seasonal changes. Seiad and Weitchpec reached similar peaks in GPP in mid-summer, but GPP at Seiad started much higher in the spring. Weitchpec had the largest seasonal changes in GPP, starting very low in the spring, reaching a summer peak, and returning to rates near 0 g O_2 m^{-2} d^{-1} by the end of October. Seasonal patterns in ER were similar to those in GPP, except that during May and June, and again during October, ER was higher at Turwar than at Weitchpec. Net ecosystem production at Turwar was always the lowest, with rates near 0 g O_2 m^{-2} d^{-1}, with slightly positive values in the spring and fall, and slightly negative values in the summer. In the spring, NEP was highest at Seiad, where it maintained a rate of ~3 g O_2 m^{-2} d^{-1} through mid-August. NEP at Seiad decreased to similar to rates as those at Turwar by the end of October. Weitchpec had moderate NEP in the spring, which increased to a peak of ~3 g O_2 m^{-2} d^{-1} in mid-summer, and then decreased until mid-September, followed by a final increase that ended the monitoring season with the highest rates of NEP.

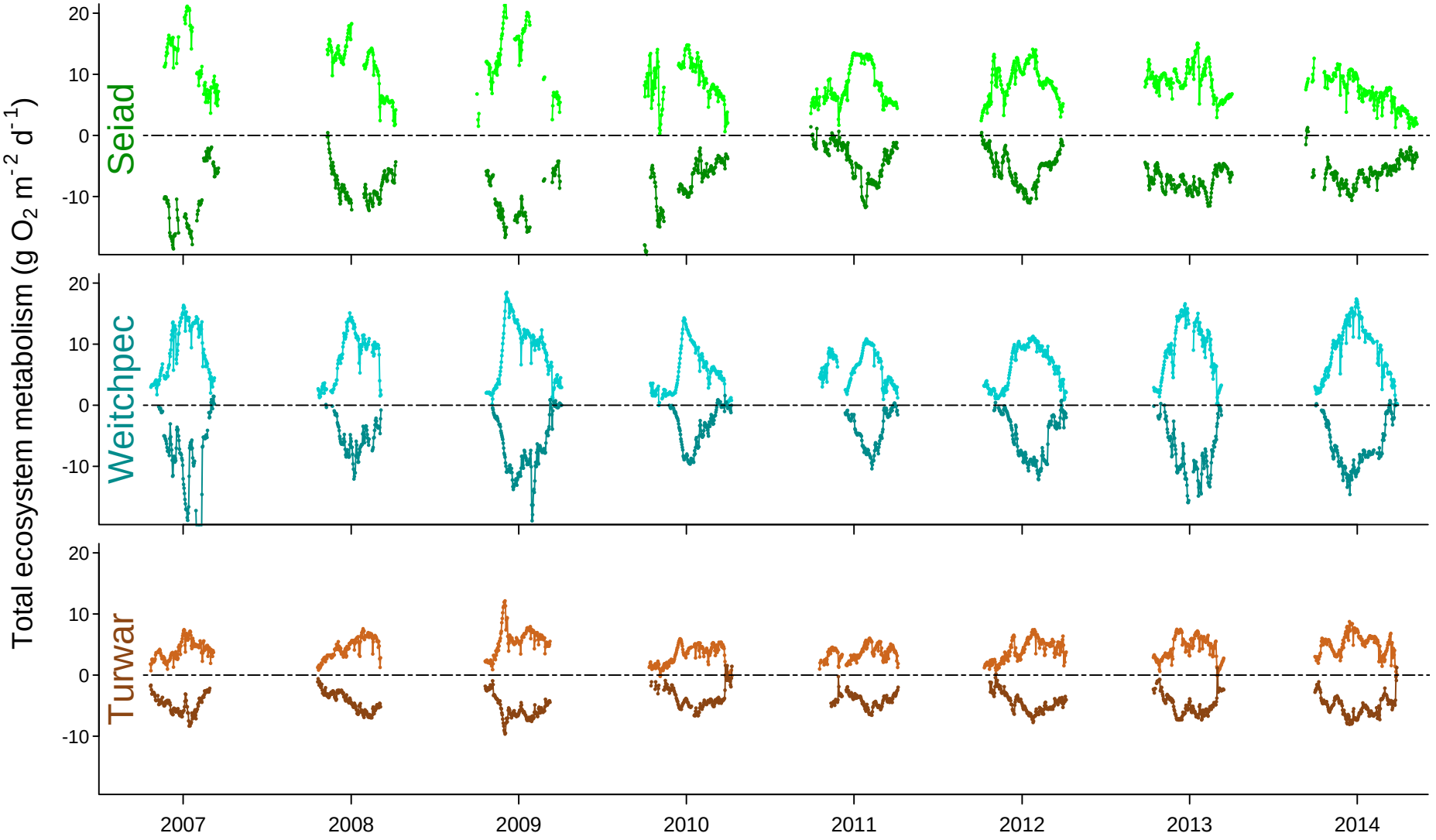

Figure 3. Time series of daily metabolism rates at Seiad, Weitchpec, and Turwar (from top to bottom) on the Lower Klamath River. Positive values shown in lighter shades are GPP and negative values shown in darker shades are ER.

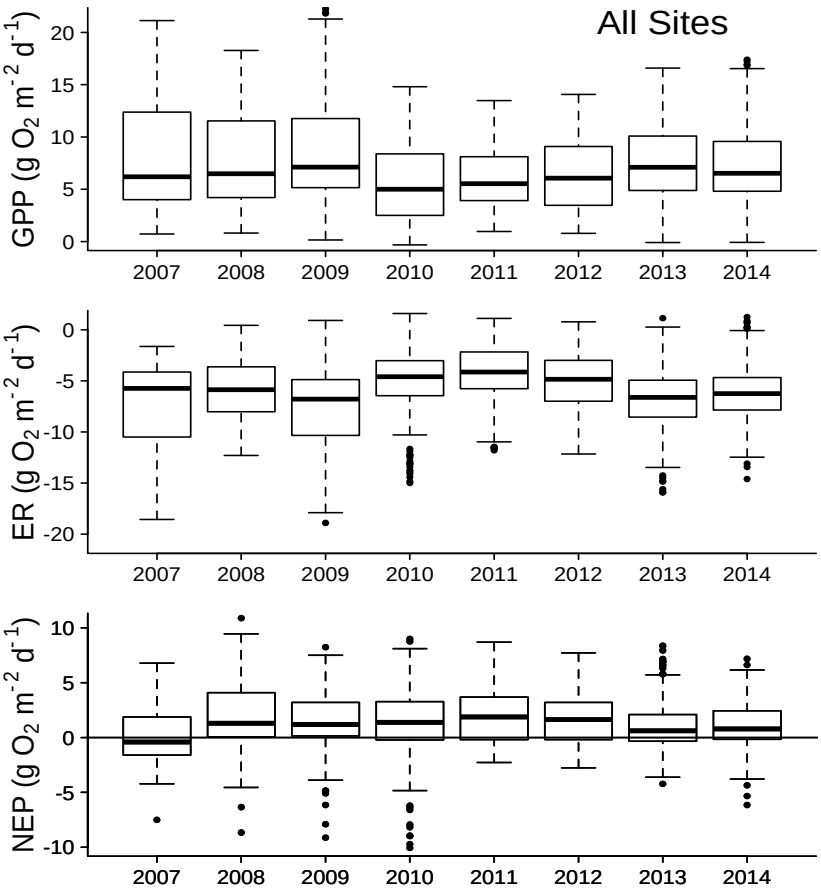

Figure 4. Box plots of GPP, ER, and NEP from three sites for May through October, on the Lower Klamath River by year.

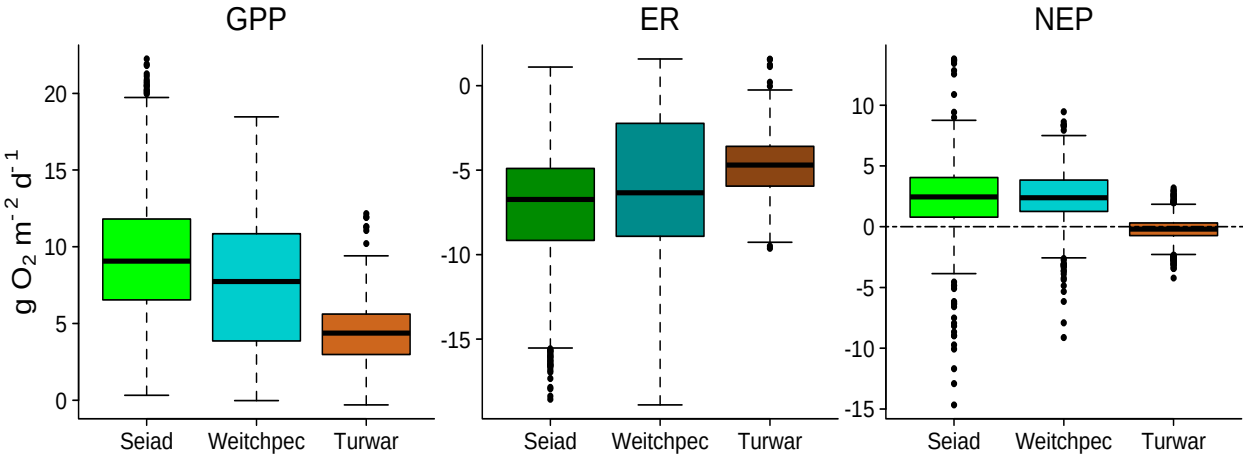

Figure 5. Box plots of GPP, ER, and NEP for May through October by site, for all eight years.

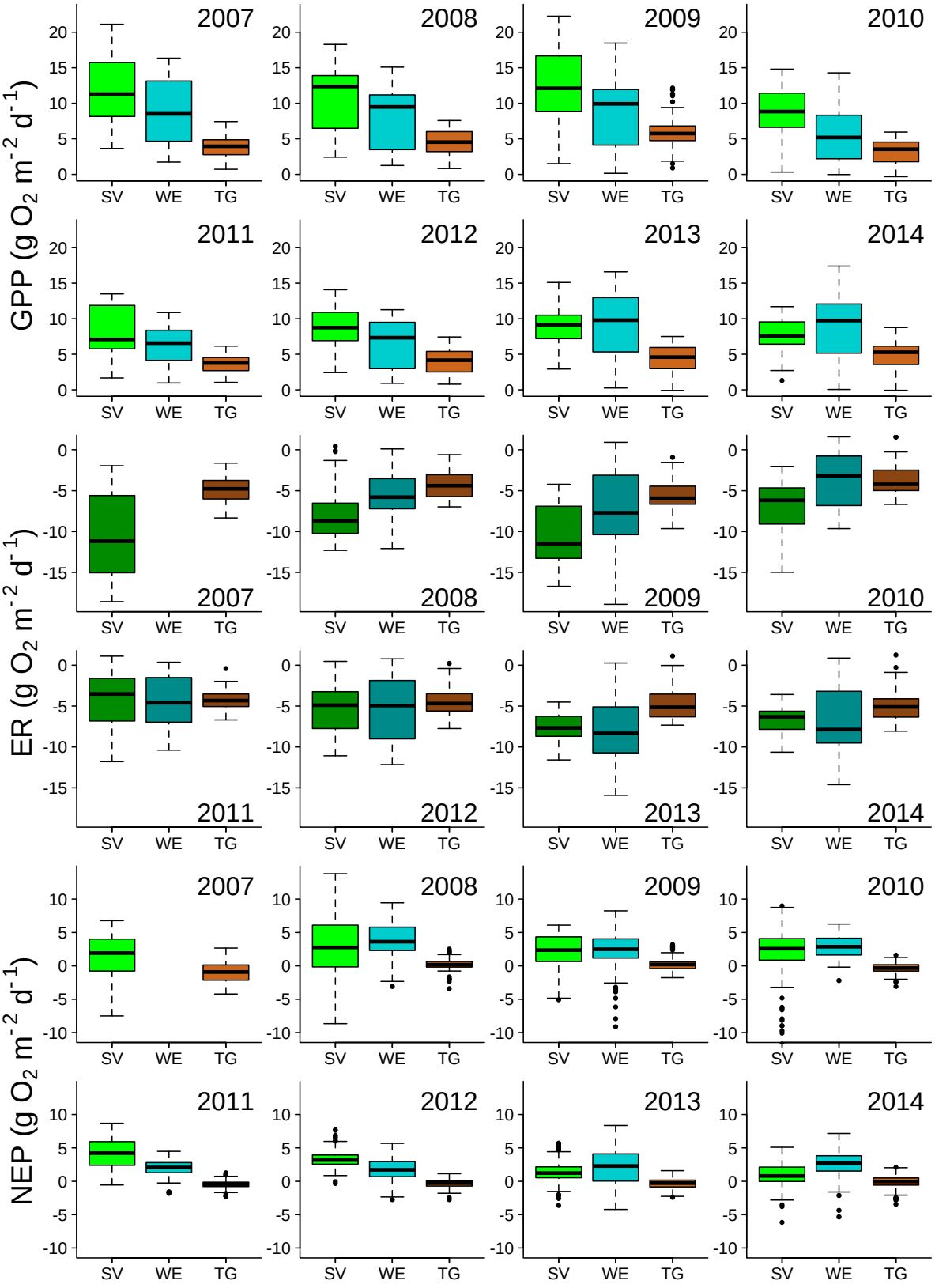

Figure 6. GPP, ER, and NEP by site and year from May–Oct. (SV=Seiad, WE=Weitchpec, TG=Turwar).

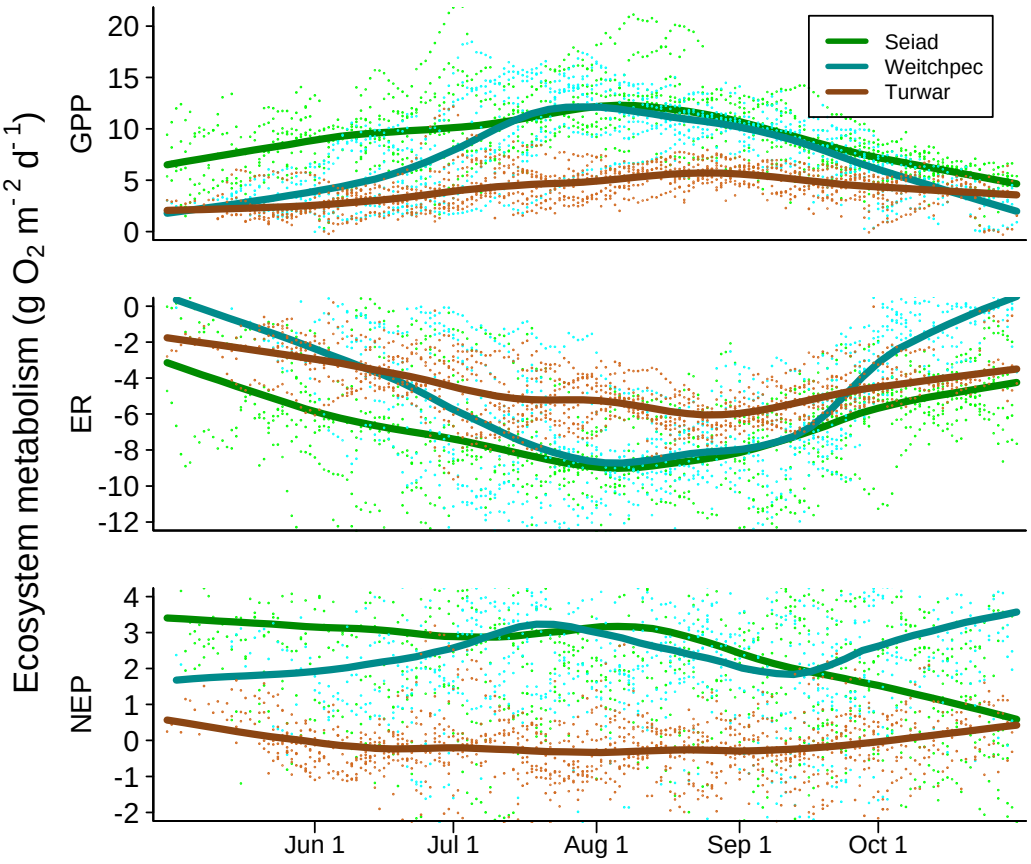

Figure 7. Generalized seasonal patterns of GPP, ER, and NEP at the three metabolism study sites based on daily metabolism data from 2007 to 2014. Points are individual days and lines are Locally Estimated Scatterplot Smoothing (LOESS) regression curves.

3.2 RELATIONSHIPS BETWEEN METABOLIC PARAMETERS, DISSOLVED O_2, AND THE CYANOBACTERIAL BLOOM

3.2.1 RELATIONSHIPS BETWEEN ECOSYSTEM METABOLISM AND MINIMUM DISSOLVED O_2

ER increased with increasing GPP at all sites during the eight-year study period (Figure 8). With all eight years of data combined, GPP explained 47%, 71%, and 72% of the variation in ER at Seiad, Weitchpec, and Turwar, respectively. From year to year, the amount that GPP explained ER was variable (

Table 3). At Seiad, only 2% of the variation in ER was explained by GPP in 2010, while 80% of the variation was explained in 2009 and 2012. At Weitchpec, variation in ER explained by GPP ranged from 49% to 85% annually, while it ranged from 22% to 86% at Turwar.

Table 3. Regression statistics for the relationship between ER and GPP by site and year on the Klamath River.

Site	Year	Slope	Intercept	*p-value*	r^2
Seiad	2007	-0.88	0.27	0.000	0.68
	2008	-0.15	-6.51	0.010	0.05
	2009	-0.66	-1.98	0.000	0.80
	2010	-0.14	-5.84	0.069	0.02
	2011	-0.72	1.86	0.000	0.55
	2012	-0.90	2.45	0.000	0.80
	2013	-0.54	-2.63	0.000	0.56
	2014	-0.47	-2.71	0.000	0.33
	All years	**-0.63**	**-1.05**	**0.000**	**0.47**
Weitchpec	2007	NA	NA	NA	NA
	2008	-0.56	-0.22	0.000	0.49
	2009	-0.85	0.98	0.000	0.65
	2010	-0.80	1.54	0.000	0.80
	2011	-0.96	1.71	0.000	0.85
	2012	-1.02	1.81	0.000	0.77
	2013	-0.77	-0.25	0.000	0.63
	2014	-0.81	0.88	0.000	0.77
	All years	**-0.83**	**1.02**	**0.000**	**0.71**
Turwar	2007	-0.47	-2.97	0.000	0.22
	2008	-0.84	-0.52	0.000	0.76
	2009	-0.73	-1.31	0.000	0.82
	2010	-0.98	-0.40	0.000	0.81
	2011	-0.79	-1.25	0.000	0.70
	2012	-0.87	-0.84	0.000	0.84
	2013	-0.91	-0.73	0.000	0.86
	2014	-0.80	-1.08	0.000	0.72
	All years	**-0.79**	**-1.13**	**0.000**	**0.73**

Autotrophic conditions (positive NEP) typically dominated at both Seiad and Weitchpec (83% and 87% of study days, respectively). In contrast, only 38% of study days were autotrophic at Turwar. At Seiad, the days with the most negative NEP (points below and furthest from the one-to-one line, Figure 8) occurred in spring 2010 during the largest discharge spike of the eight-year study period (Figure 9).

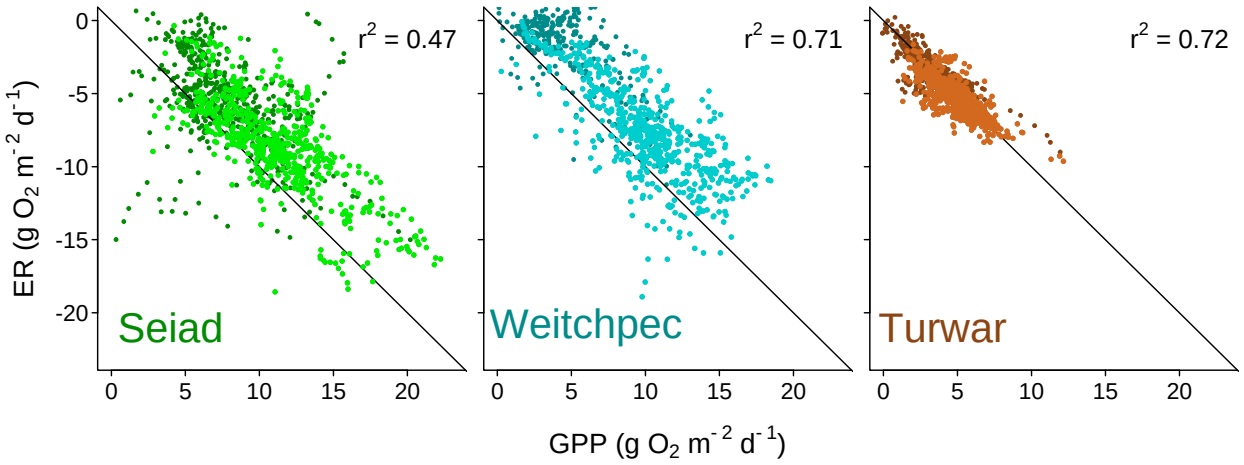

Figure 8. GPP vs. ER for the three metabolism study sites. Black line is one-to-one line, with points below the line representing heterotrophic days and points above the line representing autotrophic days. Lighter shades on each graph are summer days (July, August, September).

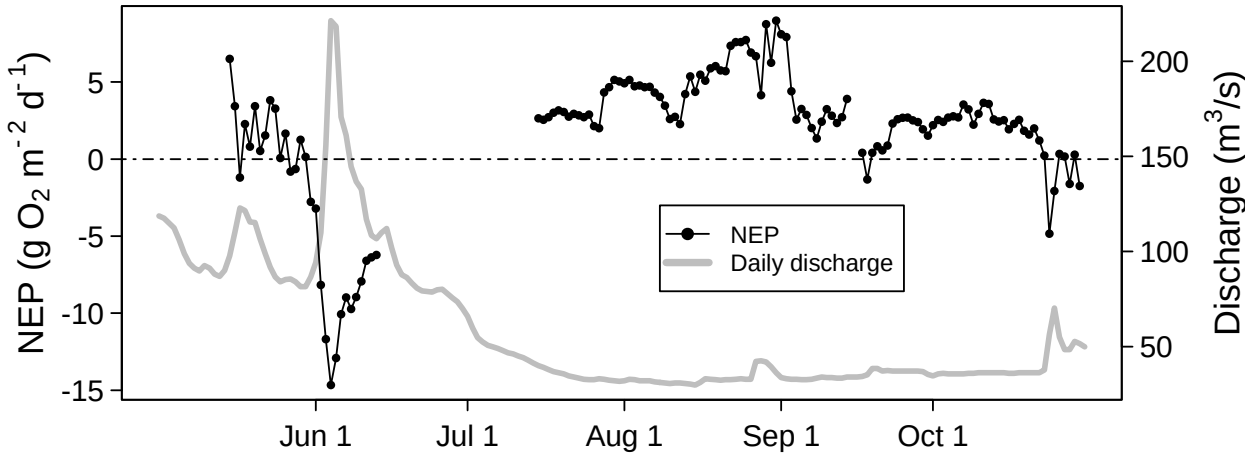

Figure 9. NEP (black line) and discharge (grey line) at Seiad during 2010.

Daily minimum dissolved O_2 saturation decreased with an increase in ER at all three sites in the Lower Klamath River[2]. The slope of the least squares regression was unique to each site, causing daily minimum dissolved O_2 saturation to dip below 90% saturation at variable rates of ER at each site (Figure 10). At Turwar, an increase in ER of 1 g O_2 m^{-2} d^{-1} resulted in a decrease of 1.8% in daily minimum dissolved O_2 saturation, with daily minimum dissolved O_2 saturation dipping below 90% at a corresponding ER of -6 g O_2 m^{-2} d^{-1}. At Weitchpec, an increase in ER of 1 g O_2 m^{-2} d^{-1} resulted in a decrease of 0.7% in daily minimum dissolved O_2 saturation, with daily minimum dissolved O_2 saturation dipping below 90% at a corresponding ER of -12 g O_2 m^{-2} d^{-1}. At Seiad, two distinct relationships occurred during different discharges. At flows below

[2] Ecosystem respiration removes dissolved O_2 from the river during mineralization of organic carbon. During the night when photosynthesis ceases, dissolved O_2 saturation reaches its lowest levels.

42 m^3/s, an increase in ER of 1 g O_2 m^{-2} d^{-1} resulted in a decrease of 1.1% in daily minimum dissolved O_2 saturation, with daily minimum dissolved O_2 saturation dipping below 90% at a corresponding ER of -9 g O_2 m^{-2} d^{-1}, but at flows above 42 m^3/s, -14 g O_2 m^{-2} d^{-1} were needed to cause minimum daily dissolved O_2 saturation to dip below 90%.

At Weitchpec and Turwar, ER alone explained a large amount of the variation in minimum daily dissolved O_2 saturation (93% and 71%, respectively). At Seiad, where the slope of the relationship between minimum dissolved O_2 and ER became different at higher rates of discharge, a model that included both ER and piston velocity (i.e., gas exchange rate per unit of river depth; minDO = 0.85×ER + 0.38×piston velocity + 93.89) had greater explanatory power (93% for ER and piston velocity model versus 83% for ER-only model).

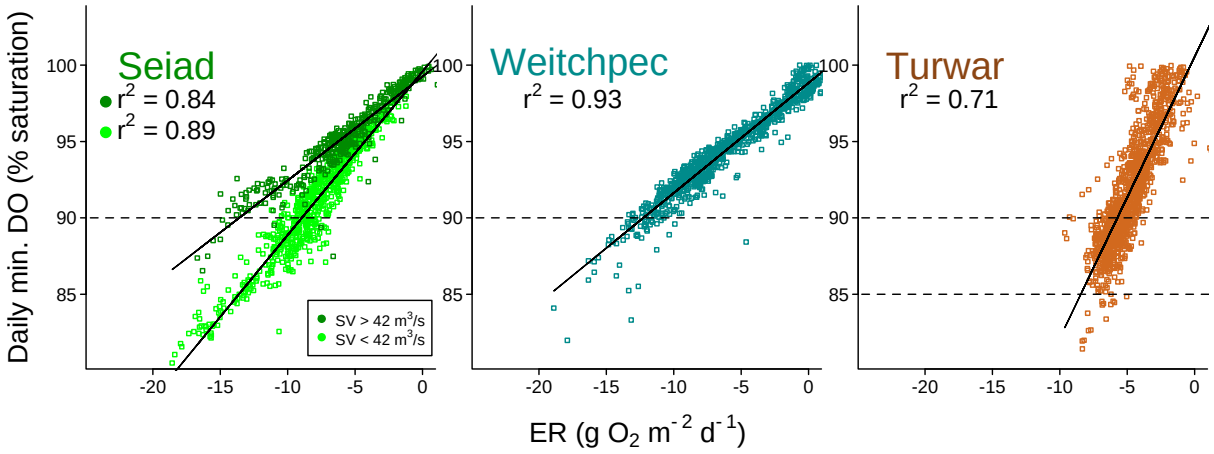

Figure 10. ER vs. daily minimum dissolved O_2 saturation (minDO). Regression slopes and constants are as follows: at Seiad when discharge < 42 m^3/s, minDO = 1.07×ER + 99.58, at Seiad at high discharge (> 42 m^3/s), minDO = 0.68×ER + 99.25, at Weitchpec minDO = 0.72×ER + 98.83 and at Turwar minDO = 1.84×ER + 100.54. A discharge of 42 m^3/s is equivalent to ~1500 ft^3/s.

As a result of the coupling of GPP and ER (Figure 8), minimum daily dissolved O_2 concentration decreased as GPP increased (Figure 11). In the Klamath River, minimum daily dissolved O_2 saturation decreased an average of 1.5%, 1.3%, and 0.7% for every increase of 1 g O_2 m^{-2} d^{-1} in GPP at Seiad, Weitchpec, and Turwar, respectively (Figure 11). The relationship was strongest at Weitchpec, where 65% of the variation in daily minimum dissolved O_2 was explained by the variation in GPP. At Seiad and Turwar, approximately 40% of the variation in daily minimum dissolved O_2 was explained by the variation in GPP. Ecosystem respiration is the strongest driver of minimum daily dissolved O_2 saturation, but because GPP is the major driver of ER, both variables are important to investigate in relation to dissolved O_2 levels.

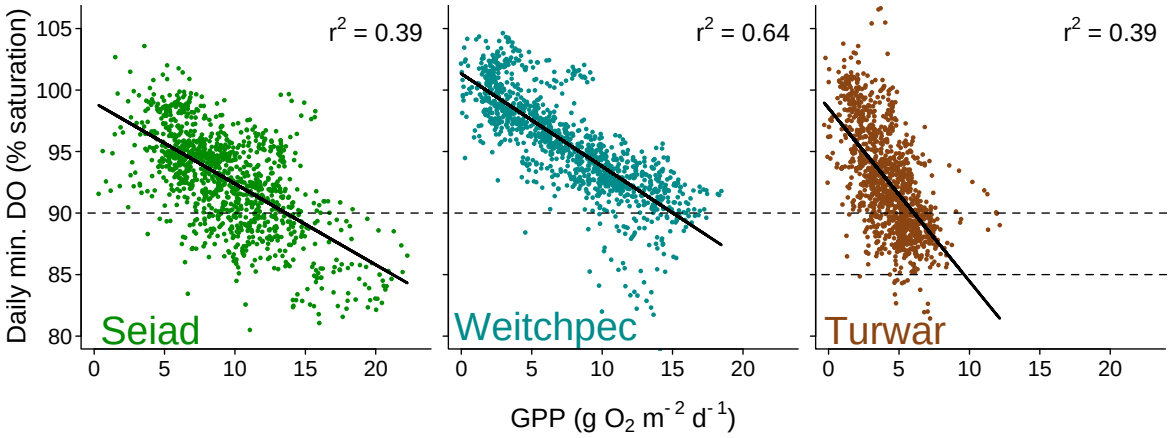

Figure 11. GPP vs. daily minimum dissolved O_2 (minDO) saturation in the Klamath River. Lines are the least squares regression indicating the relationship of minDO to GPP where minDO at Seiad = -0.66×GPP + 98.97, minDO at Weitchpec = -0.75×GPP + 101.21 and minDO at Turwar = -1.41×GPP + 98.54.

3.2.2 INFLUENCE OF CYANOBACTERIAL BLOOM ON ECOSYSTEM METABOLISM

Although the interaction effect from the ANCOVA was not significant at any site (Table 4)[3], based on regressions comparing bloom and non-bloom periods the reservoir algal bloom appeared to have affected the relationship between GPP and minimum dissolved O_2 saturation (Figure 12; Table 4). For example, the effect of the bloom on the relationship between GPP and minimum daily dissolved O_2 was significant at all sites sites (p-value = 0.000), and the lower intercept of the regression lines during bloom conditions indicates that daily dissolved O_2 values dipped lower during the bloom than during non-bloom conditions with similar rates of GPP (Figure 12). The rate of GPP required to drive minimum daily dissolved O_2 saturation below 90% was lower during non-bloom than bloom conditions by ~1.7 g O_2 m^{-2} d^{-1} at Seiad, ~3.0 g O_2 m^{-2} d^{-1} at Weitchpec, and ~0.9 g O_2 m^{-2} d^{-1} at Turwar.

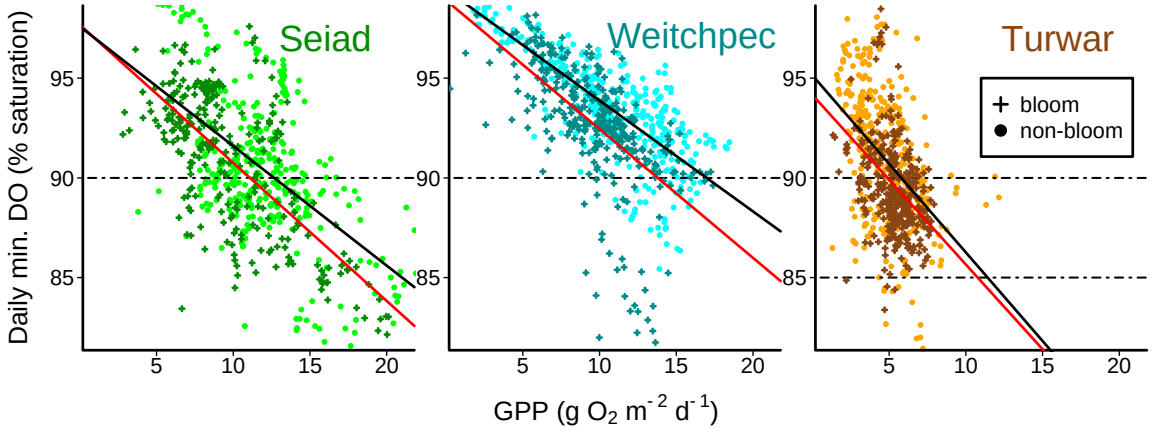

Figure 12. Daily minimum dissolved O_2 decreased with increasing rates of GPP during summer months. Daily minimum dissolved O_2 saturation was predicted by significantly lower rates of GPP during the bloom (red line, darker points) than during non-bloom conditions (black line, lighter points).

[3] Meaning that the slopes of the linear regressions of minimum daily dissolved O_2 saturation and GPP were not significantly different between bloom and non-bloom conditions

Table 4. Parameters, r^2 values, and *p-values* for the interaction effect and the additive effect of the bloom for the linear relationships between GPP and minimum daily dissolved O_2 saturation during summer months on the Klamath River.

Site	Bloom status	Slope	Intercept	r^2	*p-value: interaction effect*	*p-value: bloom effect*
Seiad	Pre-	-0.60	97.59	0.29	0.175	0.000
	During-	-0.69	97.68	0.46		
Weitchpec	Pre-	-0.56	99.45	0.61	0.071	0.000
	During-	-0.65	98.91	0.36		
Turwar	Pre-	-0.89	95.15	0.23	0.780	0.000
	During-	-0.85	94.17	0.17		

Rates of metabolism metrics shifted in variable directions and magnitudes on the Klamath River between non-bloom and bloom conditions (Table 5). There was a significant decrease in the summer means of daily GPP from non-bloom to bloom conditions at Seiad (*p-value* = 0.013), whereas the decrease in GPP at Weitchpec and the increase in GPP at Turwar was not significant. There were no significant changes in the means of daily summer ER rates between non-bloom and bloom conditions at any sites. At Seiad and Weitchpec, summer mean NEP was lower during bloom conditions than during non-bloom conditions, and there was a near significant decrease between the means of daily summer NEP from non-bloom to bloom conditions (*p-values* = 0.051 and 0.071 respectively). Turwar had an average increase in NEP of 0.1 g O_2 m^{-2} d^{-1} from daily summer non-bloom to bloom conditions and the change in the annual means of NEP from non-bloom to bloom conditions was not significant.

We found few significant differences in the means of metabolism metrics between the 10 days before a major bloom spike and the 10 days following (and including) the major bloom spike (Table 6). We looked at the 10 days before and during a bloom spike in an attempt to isolate the effects of the bloom and reduce other seasonal effects on metabolism. We conducted a t-test (paired by year) to compare the means of the 10 days of GPP, ER and NEP before and during the bloom spike for 2010-2014, which are the years that the phycocyanin sensors showed an obvious shift from non-bloom to bloom conditions (Appendix A). Although there was a decrease in GPP rates at all sites from pre-bloom to bloom conditions, only Turwar had a statistically significant decrease in the means by year of non-bloom to bloom conditions (CI = 0.2-1.2, *p-value* = 0.020). The direction of shifts in ER and NEP were not consistent at all sites and, and no significant changes occurred in the means of non-bloom to bloom conditions.

Table 5. Summer (Jul, Aug, Sep) means of metabolism metric by site and year during pre-bloom (Pre-) and post bloom-onset (Post-) conditions, and means across all years. Grey highlight indicates a statistically significant change in the summer means of metabolism metrics from pre- to post- bloom conditions (paired t-test by year).

		GPP		ER		NEP	
Site	Year	Pre-	Post-	Pre-	Post-	Pre-	Post-
Seiad	2007	16.8	8.1	-15.3	-6.9	1.5	1.2
	2008	13.8	12.5	-9.5	-10.3	4.3	2.2
	2009	21.3	16.1	-16.0	-12.9	5.3	3.2
	2010	12.3	9.1	-8.2	-5.5	4.1	3.6
	2011	10.6	10.5	-5.2	-7.7	5.4	2.8
	2012	11.2	9.0	-8.4	-5.4	2.9	3.6
	2013	10.4	8.2	-8.4	-8.3	2.0	-0.1
	2014	9.1	7.0	-9.1	-6.7	0.0	0.3
	mean	**12.0**	**9.8**	**-8.9**	**-7.8**	**3.1**	**2.0**
Weitchpec	2007	12.4	9.6	NA	NA	NA	NA
	2008	10.7	10.2	-5.9	-6.4	4.8	3.8
	2009	16.4	11.2	-10.3	-10.0	6.1	1.2
	2010	8.7	6.6	-6.0	-3.9	2.7	2.7
	2011	6.1	8.9	-3.8	-7.5	2.3	1.4
	2012	9.1	8.9	-7.1	-8.7	2.0	0.1
	2013	13.1	7.5	-10.6	-8.6	2.5	-1.0
	2014	13.8	11.4	-11.5	-8.3	2.3	3.1
	mean	**10.7**	**9.7**	**-7.5**	**-7.9**	**2.9**	**1.9**
Turwar	2007	4.7	4.4	-6.0	-3.9	-1.3	0.7
	2008	4.6	6.1	-3.8	-6.0	0.8	0.1
	2009	7.4	6.2	-7.1	-6.2	0.3	0.0
	2010	4.0	4.2	-4.5	-5.0	-0.4	-0.8
	2011	3.1	4.9	-3.6	-5.5	-0.6	-0.6
	2012	4.8	5.2	-5.3	-5.7	-0.5	-0.4
	2013	5.9	4.3	-6.2	-4.9	-0.3	-0.6
	2014	7.0	5.5	-7.1	-5.8	-0.1	-0.3
	mean	**4.9**	**5.3**	**-5.3**	**-5.4**	**-0.4**	**-0.2**

Table 6. Means of metabolism metric by site and year for 10 days prior to a bloom spike (Pre-) and post/during-bloom spikes (Post-), and means across all years. Grey highlight indicates a statistically significant change in the 10-day means of metabolism metrics from Pre- to Post- bloom spikes (paired t-test by year).

		GPP		ER		NEP	
Site	Year	Pre-	Post-	Pre-	Post-	Pre-	Post-
Seiad	2010	11.3	11.2	-5.2	-4.2	6.1	7
	2011	12.8	12.7	-10.8	-7.3	2	5.4
	2012	12.1	8.5	-8.2	-5.1	3.8	3.4
	2013	10.6	11.8	-8.6	-10.9	2	0.9
	2014	10.0	9.3	-9.5	-8	0.6	1.3
	mean	**11.4**	**10.7**	**-8.5**	**-7.1**	**2.9**	**3.6**
Weitchpec	2010	9.4	7.8	-7	-4.7	2.4	3.1
	2011	10.3	10	-7.5	-8.8	2.8	1.2
	2012	10.1	9.1	-10.4	-9.3	-0.4	-0.2
	2013	10.1	10.3	-8.8	-11.6	1.4	-1.3
	2014	14.7	15.8	-10.7	-10.5	4	5.3
	mean	**10.9**	**10.6**	**-8.9**	**-9**	**2**	**1.6**
Turwar	2010	4.7	4.4	-6.3	-5.2	-1.6	-0.8
	2011	5.3	4.9	-5.7	-6	-0.3	-1.1
	2012	6.6	5.6	-6.7	-5.8	-0.1	-0.3
	2013	5.8	4.5	-6.2	-5.4	-0.3	-0.8
	2014	7.2	6.6	-7	-6.6	0.3	0
	Mean	**5.9**	**5.2**	**-6.4**	**-5.8**	**-0.4**	**-0.6**

3.3 ENVIRONMENTAL DRIVERS OF GPP AND ER

3.3.1 INTER-ANNUAL CORRELATION ANALYSIS

Rates of GPP and ER were generally low in the spring and fall (Figure 3, Figure 7) when higher flows occurred. During base flow conditions sites tended to experience a full range of GPP rates, whereas during higher flows GPP was generally confined to lower rates (Figure 13). This pattern was most pronounced at Weitchpec, followed by Turwar, with Seiad deviating from this pattern during some years. Scatterplots of GPP vs. discharge show a seasonal progression, where GPP increased as flow decreases in May through July and then GPP decreased as flow increased again in September and October (Figure 13). Because the lowest discharge generally occurs from the months of July-September, we focused our analysis of inter-annual patterns of these three months, which we referred to as the summer.

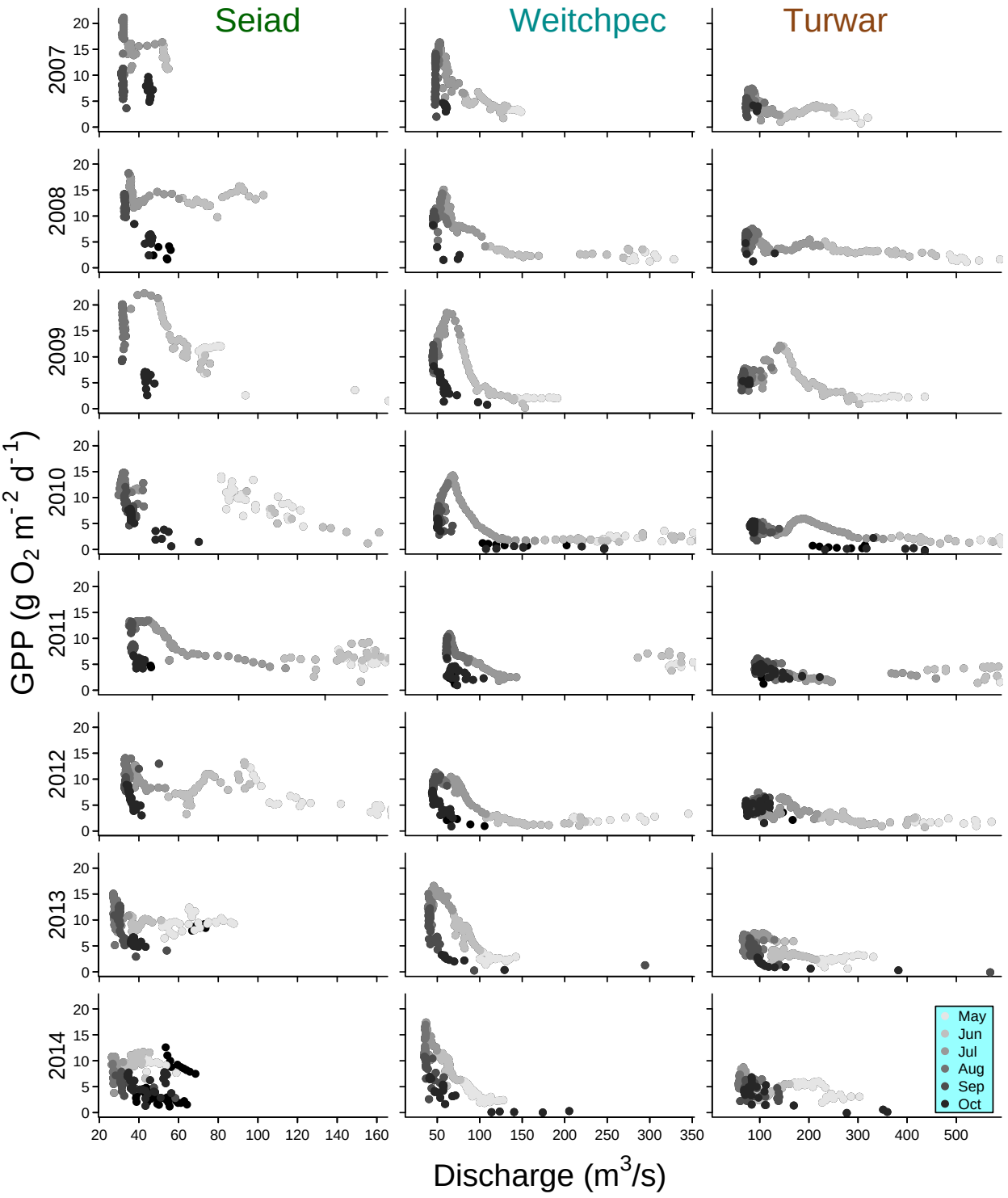

Figure 13. GPP vs. discharge. Lighter grey is earlier in the season, darker grey is later in the season.

Summer means of metabolism metrics were related to mean summer base-flow on the Klamath River. Means of daily summer GPP and ER decreased with increasing mean summer base-flow at Weitchpec and Turwar, and mean summer ER was generally a reflection of GPP (Figure 14, Figure 15). At Seiad, there were no statistically significant relationships between mean summer base-flow and GPP or ER. At Weitchpec and Turwar, 2009, 2013, and 2014 had the highest summer rates of GPP, whereas at Seiad, 2009 had the highest rate of GPP but 2013 and 2014 had the lowest rates of GPP. Mean NEP increased with increasing base-flow at Seiad, but were not associated with base-flow rates at Weitchpec or Turwar (Figure 14).

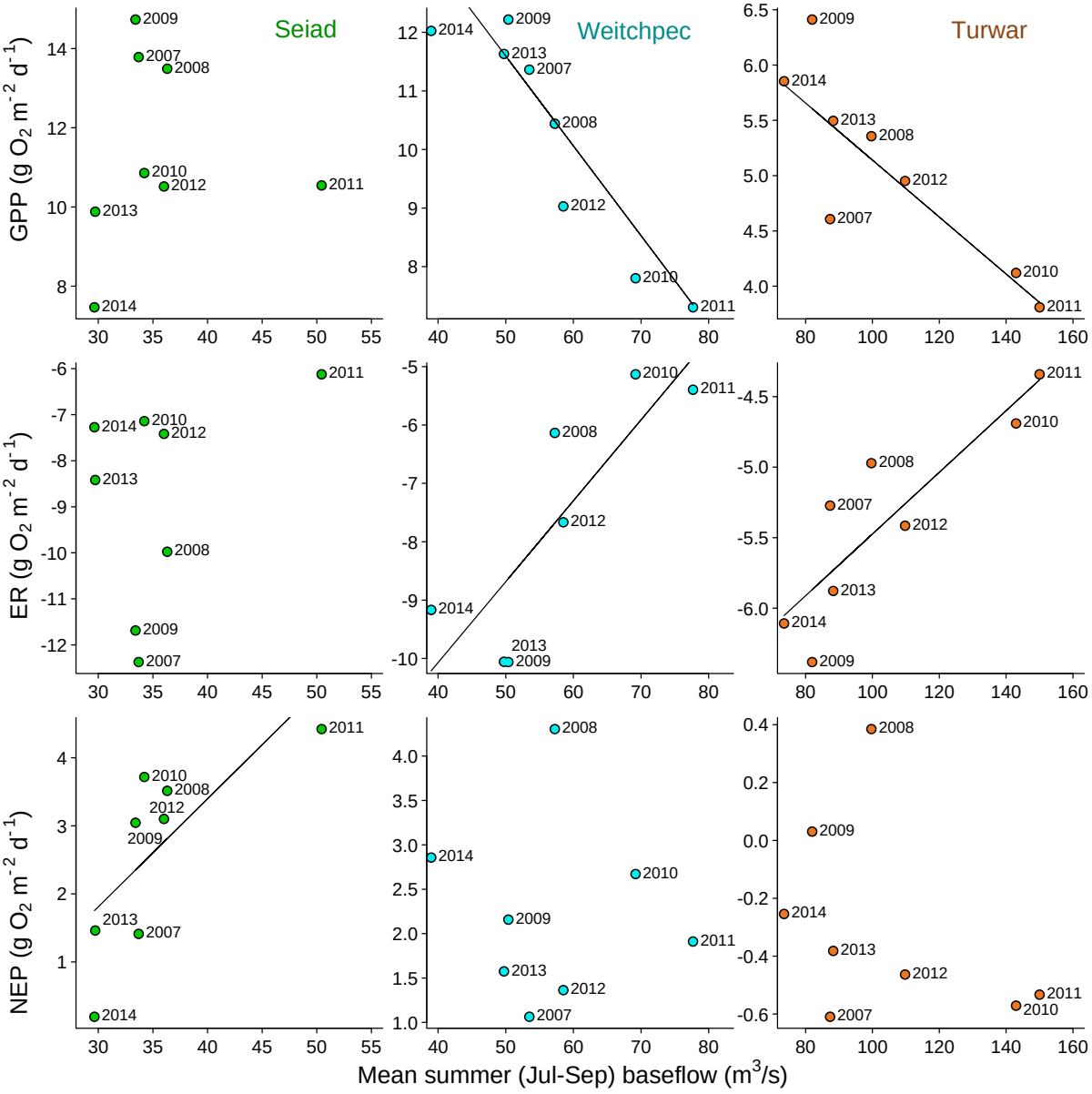

Figure 14. Summer (Jul-Sep) mean metabolism parameters by summer base-flow at each study site. Each point represents the mean of daily summer measurements for one season. Lines are least squares regressions (shown only when statistically significant) where mean summer GPP at Weitchpec = -0.15×Q + 18.74, mean summer GPP at Turwar = -0.3×Q + 7.84, mean summer ER at Weitchpec = 0.14×Q – 15.61, mean summer ER at Turwar = 0.02×Q – 7.66 , and mean summer NEP at Seiad = 0.16×Q – 2.95.

Relationships between mean summer base-flow and metabolism metrics were evident among sites, in addition to within sites (Figure 15). GPP decreased exponentially with increasing mean summer base-flow within and among sites. Outliers from 2013 and 2014 at Seiad (Figure 14), where GPP was uncharacteristically low compared to other years, deviated from this relationship. ER also decreased with increasing base-flow, but increased scatter in the residuals at lower rates of discharge (i.e., at Seiad and Weitchpec) make the relationship more difficult to characterize. NEP generally decreased among sites from upstream to downstream, and by base-flow from low to high, but at Seiad, NEP increased with increasing base-flow. Seiad was the only site with a significant relationship between NEP and base-flow rates (Figure 14).

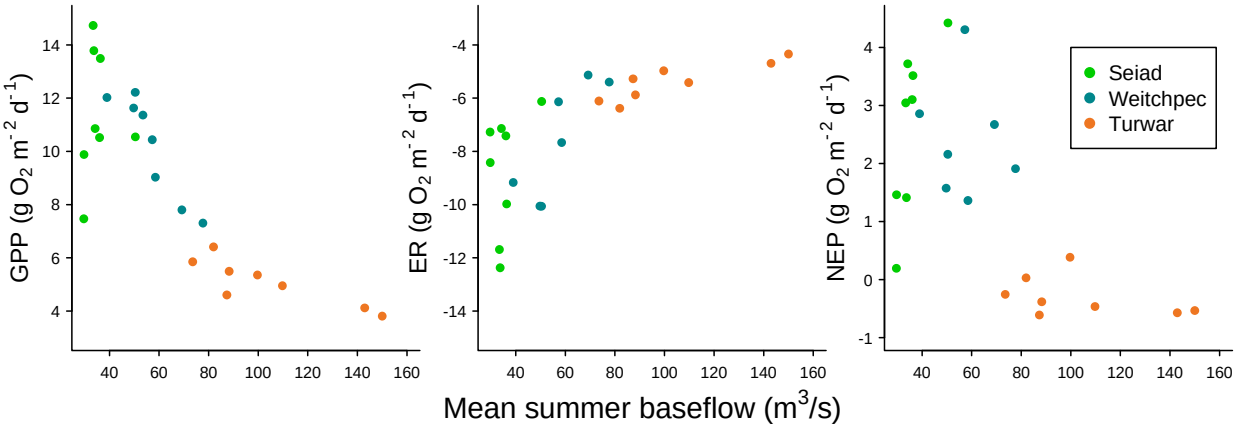

Figure 15. GPP, ER, and NEP vs. mean summer base-flow.

Many environmental variables that may relate to rates of metabolism on the Klamath River were highly correlated with mean summer base-flow at the summer seasonal scale (Table 7). The proportion of discharge originating from Iron Gate Dam, mean June discharge, and mean depth were are all correlated to mean summer base-flow with an R^2 value of 0.92 or higher at each site, and 0.90 or higher among sites. The size of the largest flood was the only discharge metric that was not highly correlated with mean summer base-flow within sites. Water temperature and nutrients, with the exception of NO_3, was highly correlated with mean summer base-flow rates within sites and among sites (r^2 = 0.64 – 0.92). Chl. a, NO_3 and total suspended solids were not highly correlated with mean summer base-flow within or among sites (r^2 = 0.09 – 0.58).

Summer means of environmental variables that were not highly correlated (Pearson's correlation coefficient < 0.60, Table 7) with mean summer base-flow were not strong predictors of summer metabolism. There were no significant linear relationships between summer mean total suspended solids or Chl. a and summer mean metabolism metrics at any of the sites. The size of winter floods may influence rates of ecosystem metabolism. At Seiad, there was a negative relationship between the size of the largest winter flood and mean summer GPP and ER, although the relationship was not statistically significant (Figure 16). Weitchpec and Turwar did not show a relationship between size of maximum winter flood and GPP or ER. Because NO_3 was the only measured nutrient variable in this analysis that had a lower correlation with summer base-flow within sites, it was the only one that we considered. At Weitchpec, NEP decreased

with increasing NO_3 concentrations (*p-value* = 0.020), but no other sites had significant relationships with NO_3.

Mean summer SRP decreased exponentially with increasing base-flow and this relationship was evident within and among sites (Figure 17). Nitrate concentrations also decreased with increasing base-flow, but the relationship was less evident within sites, and was more variable than the relationship between SRP and base-flow.

Table 7. Pearson's correlation coefficients between mean summer annual base-flow and summer means of other environmental variables on the Klamath River by site and with all sites combined for years 2007-2014.

	Mean summer base-flow			
	Seiad	Weitchpec	Turwar	All Sites
% Q from Iron Gate Dam	-0.97	-0.99	-0.97	-0.90
Mean June Q	0.92	0.95	0.96	0.91
Max water-year flood	0.39	-0.24	-0.15	0.72
Mean water temperature	-0.69	-0.84	-0.76	-0.66
Total phosphorus	-0.80	-0.90	-0.72	-0.80
Soluble reactive phosphorus	-0.77	-0.92	-0.77	-0.80
Nitrate	0.09	-0.22	-0.58	-0.48
Total nitrogen	-0.64	-0.85	-0.86	-0.81
Chl. a	-0.43	-0.44	-0.55	-0.51
Total suspended solids	0.22	-0.37	-0.16	-0.29
Mean depth	0.99	0.97	1.00	0.96

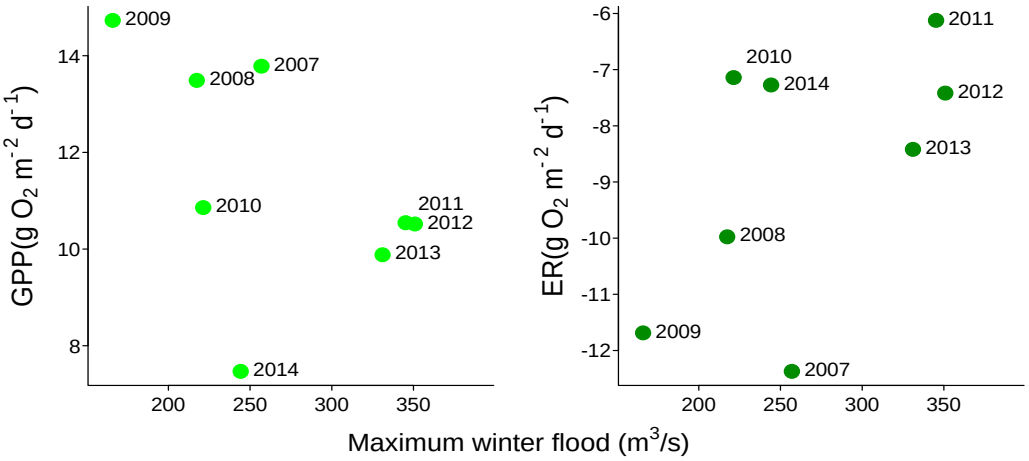

Figure 16. Mean summer GPP and ER vs. maximum winter flood. Relationships were not statistically significant.

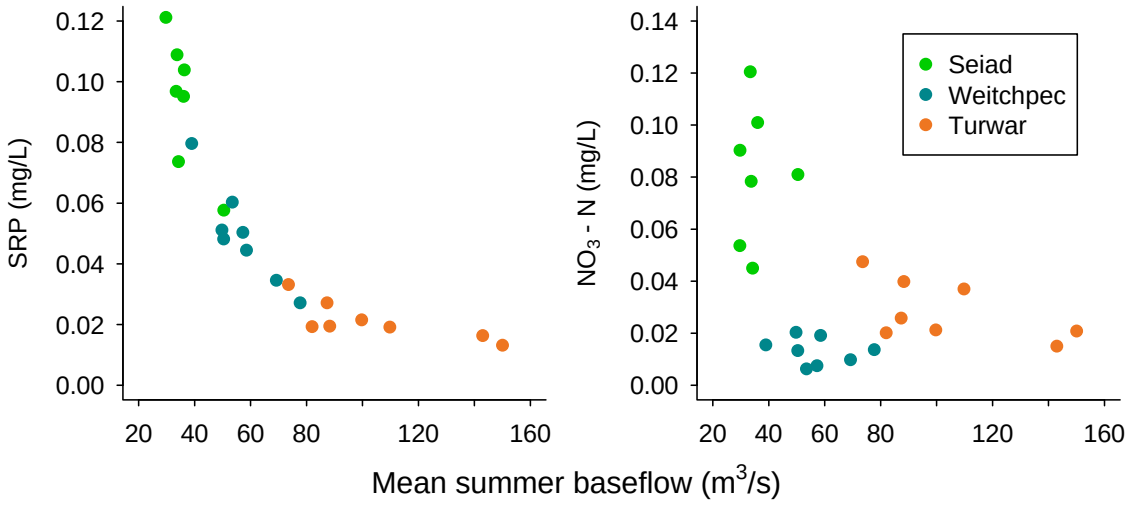

Figure 17. Mean summer SRP and NO_3 vs. mean summer base-flow.

3.3.2 DAILY TIME SERIES MODELS TO EVALUATE INTRA-ANNUAL CONTROLS ON GPP

We used multivariate time series models with the fraction of flow from Iron Gate Dam, light, algal bloom status, and an autocorrelation coefficient to predict daily variation in GPP. We included the above parameters in the model to test the extent to which these factors influenced the seasonal trends in GPP (Figure 3). We assessed the extent to which the fraction of flow from Iron Gate co-varied with parameters that may in part control GPP.

The model parameter θ, which represents the degree of auto-correlation in daily GPP, was > 0.5 most years, indicating a strong degree of auto-correlation (Appendix C). Means of the θs for all years for each site ranged from 0.70 at Turwar to 0.73 at Seiad. 2014 had a much lower θ value than previous years at Seiad and Turwar, and both 2014 and 2013 were low at Weitchpec, indicating lower autocorrelation in daily GPP during recent years.

We assessed model qualitatively and quantitatively. We plotted the time series of GPP from the model with the time series of the measured GPP data for each site and year (Figure 18, Appendix D). Rates of modeled GPP that are similar to rates of calculated GPP signify that the model parameters (light, fraction of discharge from Iron Gate, bloom status, and the autocorrelation coefficient) were the primary controls on within-season GPP. Where the modeled GPP deviated from the measured GPP, other factors controlled variation in GPP. We can use the situations where modeled GPP deviated from measured GPP to hypothesis what additional factors may be controlling GPP.

We assed the accuracy to which the model predicted GPP by by plotting the modeled GPP by the calculated rates of GPP at each site. Modeled GPP using predicted light (that did not take into account cloud cover) explained 79%, 76%, and 27% of the variation in measured GPP at Seiad, Weitchpec, and Turwar respectively (Figure 19). Using measured solar radiation in the model

improved the predictive ability of the model over using modeled light, where the model explained 82% of the variation in measured GPP at Weitchpec.

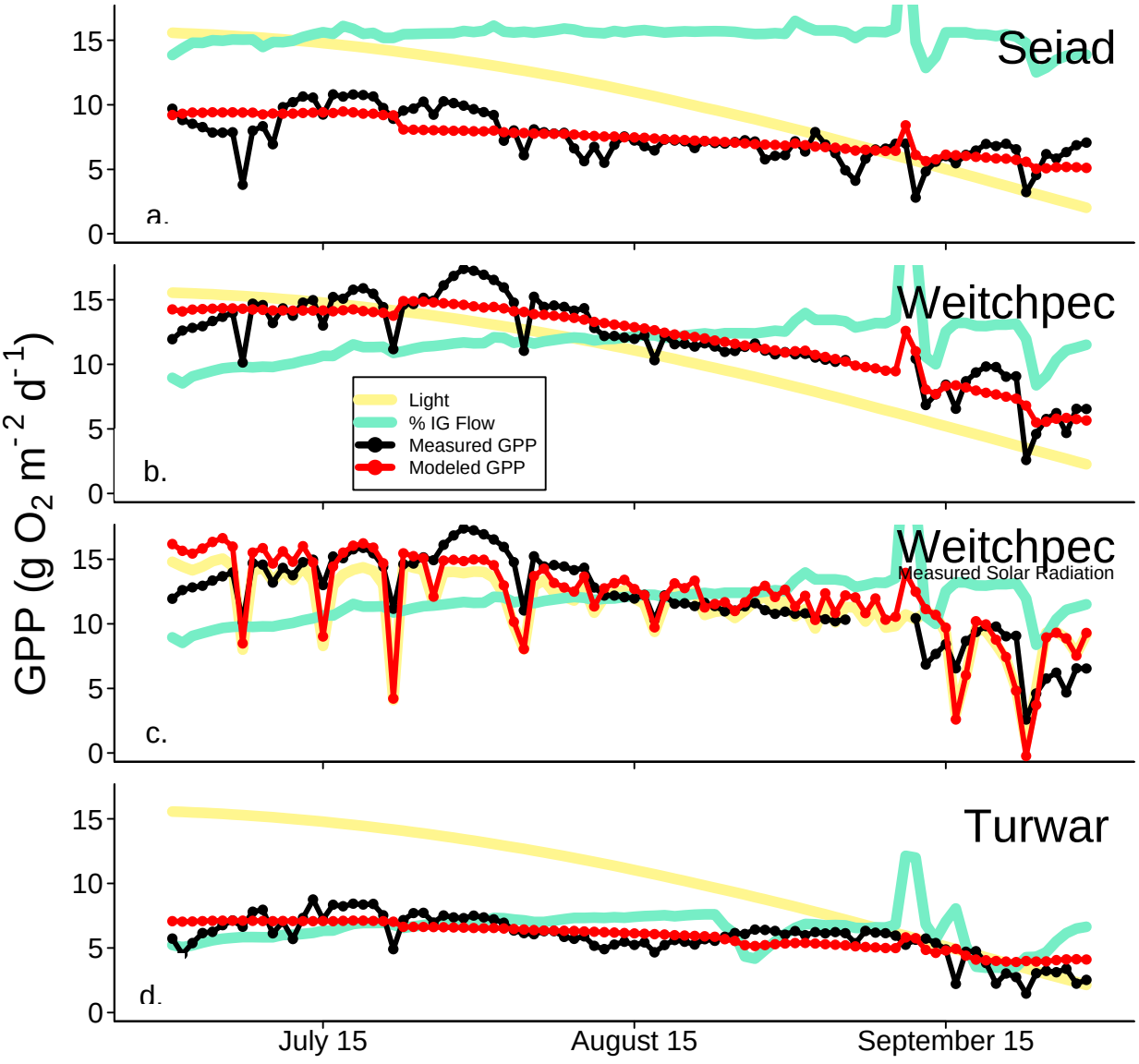

Figure 18. Seasonal trends in rates of modeled GPP (red line) from the multivariate time series model and rates of measured GPP for 2014 (black line). The yellow line represents relative light conditions resulting from changes in day length (panels a., b., and d.) and daily solar radiation measurements, which represent both day length and cloud cover (panel c.). The green line represents the fraction of flow from Iron Gate. Scales for fraction of flow from Iron Gate and light are arbitrary and are used to show trends in these variables.

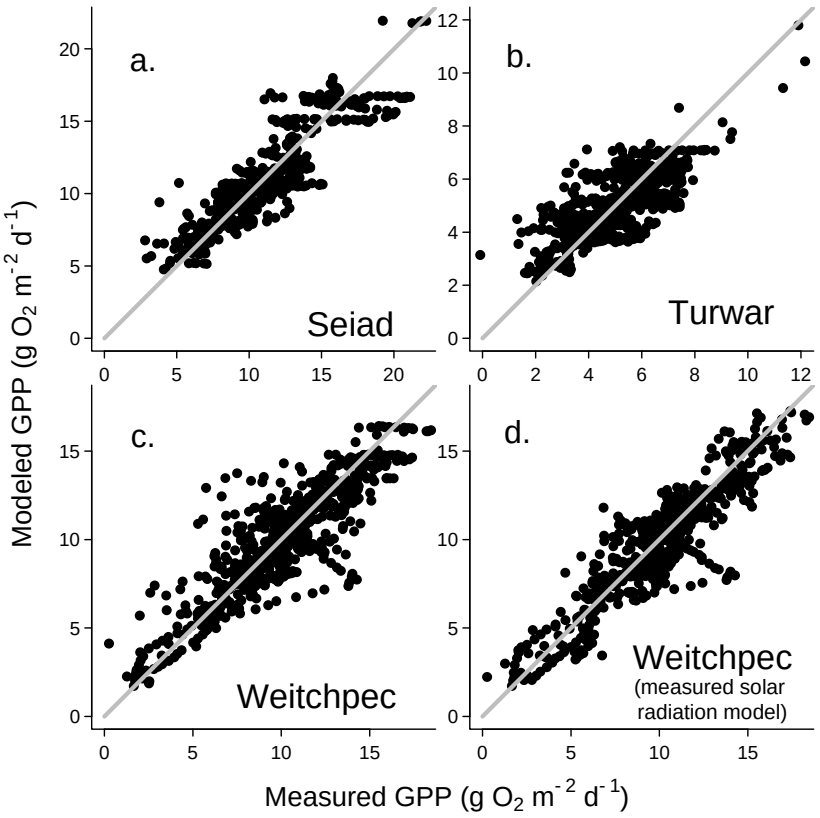

Figure 19. Modeled GPP vs. measured GPP at all sites. Grey line is the one-to-one line.

Daily rates of GPP were influenced by light, fraction of discharge from Iron Gate, and the presence of algae blooms in the Klamath River (Figure 20). At Seiad, the highest rates of GPP were predicted to occur when the fraction of discharge from Iron Gate was high (0.94; 95th quantile of summer discharge ratio) and during high light (i.e., longest days), and not during the presence of an algal bloom (Equation 4). During bloom conditions at similar light and fraction of discharge from Iron Gate, we predicted GPP to decrease ~3.5 g O_2 m^{-2} d^{-1}. With low fraction of discharge from Iron Gate (0.55; 5th quantile of summer discharge ratio) and no algal bloom, we predicted a similar decrease of ~3.5 g O_2 m^{-2} d^{-1}. We predicted GPP to be lowest when there was an algal bloom and fraction of discharge from Iron Gate was high; a condition that would drive GPP ~7 g O_2 m^{-2} d^{-1} lower than at low fraction of discharge from Iron Gate and no bloom conditions, at a given light level. The predicted increase in GPP from low to high light conditions was ~3 g O_2 m^{-2} d^{-1}.

At Weitchpec, light and fraction of discharge from Iron Gate were associated with GPP (Figure 20). We tested two models at Weitchpec; one using predicted light and the other model incorporated measured solar radiation. With both models, the presence of the algal bloom lowered predicted GPP by ~1-2 g O_2 m^{-2} d^{-1} while other conditions were the same. The model with measured solar radiation, which takes into account weather conditions such as clouds and smoke, had a steeper slope than the model that used modeled light (i.e., day length), indicating sensitivity of GPP to variation in light. GPP was spread across a wider range of light conditions

when using solar radiation as a predictor compared to modeled light. In the model with predicted light, lowering the fraction of discharge from Iron Gate from 0.72 to 0.26 (the 95th and 5th quantiles of the summer-time discharge ratios across all years), lowered the predicted GPP by ~9 g O_2 m^{-2} d^{-1} during respective bloom conditions. The model with measured solar radiation predicted GPP to decrease by ~6 g O_2 m^{-2} d^{-1} under the same change in the Iron Gate discharge ratio.

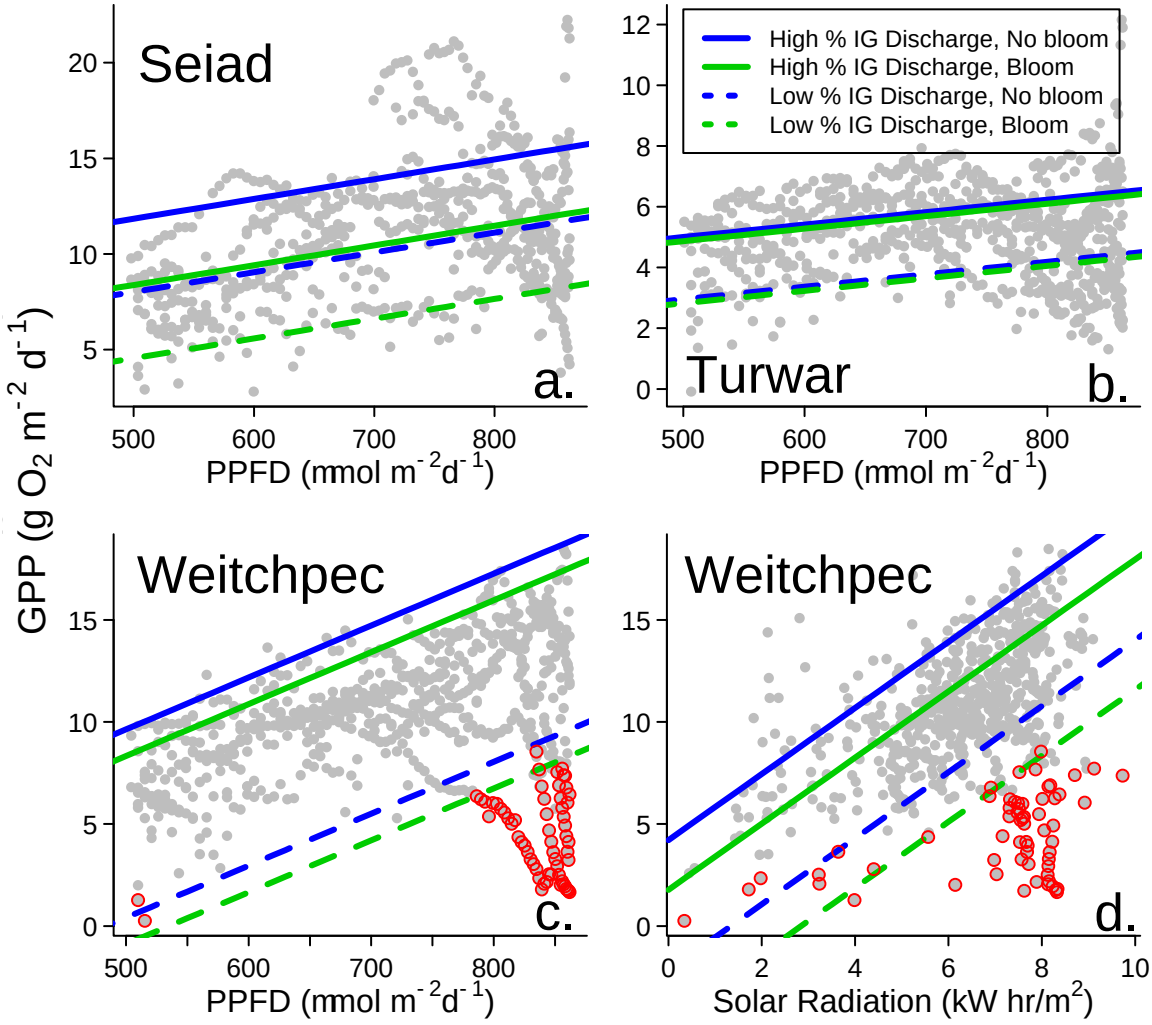

Figure 20. GPP vs. predicted light (photosynthetic photon flux density; PPFD) each site (panels a., b., and c.), and GPP vs. measured solar radiation at Weitchpec (panel d.) which included a second model using data from a nearby light sensor. Scenarios are based on mean parameter estimates for all years. Grey dots are measured GPP from all years and lines correspond to predictions of GPP under conditions of high fraction of discharge from Iron Gate without algal bloom (solid blue line), high fraction of discharge from Iron Gate with algal bloom (solid green line), low fraction of discharge from Iron Gate with no algal bloom (dashed blue line), low fraction of discharge from Iron Gate with algal bloom (dashed green line). Red points at Weitchpec are high flow days (> 90th quantile of summer discharge).

At Turwar, the predicted decrease in GPP due to the algal bloom was small (Figure 20). Changing the fraction of discharge from Iron Gate from 0.43 to 0.12 (the 95th and 5th quantiles of summer discharge ratios) resulted in a decrease in predicted GPP of ~2 g O_2 m^{-2} d^{-1}. The increase in predicted GPP from short to long days during the summer was ~1 g O_2 m^{-2} d^{-1}.

Water column nutrient concentrations increased within and among sites as the fraction of flow originating from Iron Gate increased on the Klamath River. The relationships between nutrients concentrations (samples taken every two weeks) and the fraction of flow from Iron Gate was unique to each nutrient parameter but similar among sites (Figure 21). NO_3 increased on some dates as the fraction of flow from Iron Gate increased, but NO_3 remained near detection over the range of discharge ratios as well. Total nitrogen increased with increasing fraction of flow from Iron Gate, although higher variability existed at higher discharge ratios. Total phosphorus and SRP increased exponentially as fraction of flow from Iron Gate increased. These relationships were evident within and among site, with these plots showing a strong longitudinal trend (Figure 21).

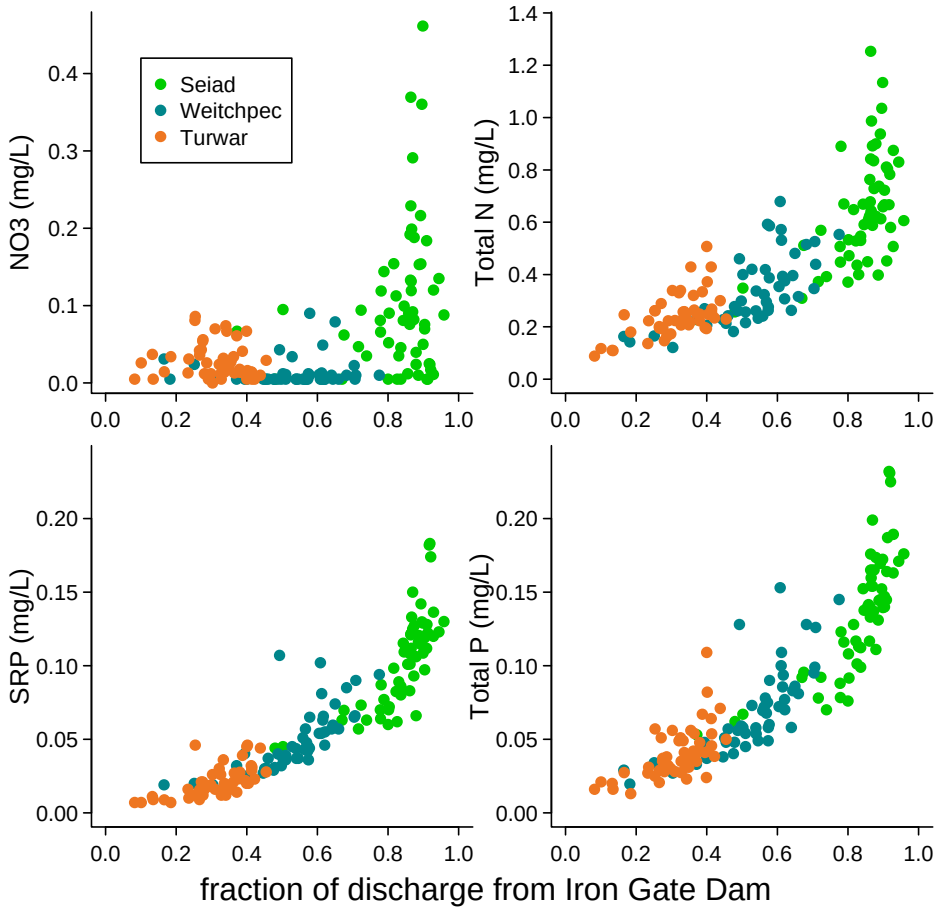

Figure 21. Nutrients concentrations (samples taken every two weeks) during the summer vs. fraction of discharge from Iron Gate Dam for all years of study at Seiad (green), Weitchpec (blue), and Turwar (brown).

The time series model predicted GPP to increase with an increase in the fraction of flow from Iron Gate Dam, but pulse releases from Iron Gate Dam that cause a temporary increase in the fraction of flow from Iron Gate may cause a short-term decrease in GPP rates. Decreases in daily summer rates of GPP associated with increased flow from Iron Gate Dam were small and difficult to dectect. We plotted the discharge from Iron Gate in the late summer during even-numbered years during pulse realeases with daily GPP to visually assess the effects the pulse may have had on short-term rates of GPP. These plots indicate that summer discharge pulses from Iron Gate were associated with a temporary, small decrease to GPP during some years (Figure 22). GPP at Seiad decreased one to two days following increases in discharge from Iron Gate dam and GPP at Weitchpec decreased two to three days after the increased discharge release (in 2012 and 2014), as expected due to water travel time (Figure 22). Cloud cover and missing GPP data, which coincided with pulse-flow events made it difficult to isolate the effects of the pulse from the effects of decreased solar radiation, and it appears that decreases in solar radiation may have caused larger decreases in GPP than the pulse flows (seen when GPP decreased at all sites on the same day as decreases in light).

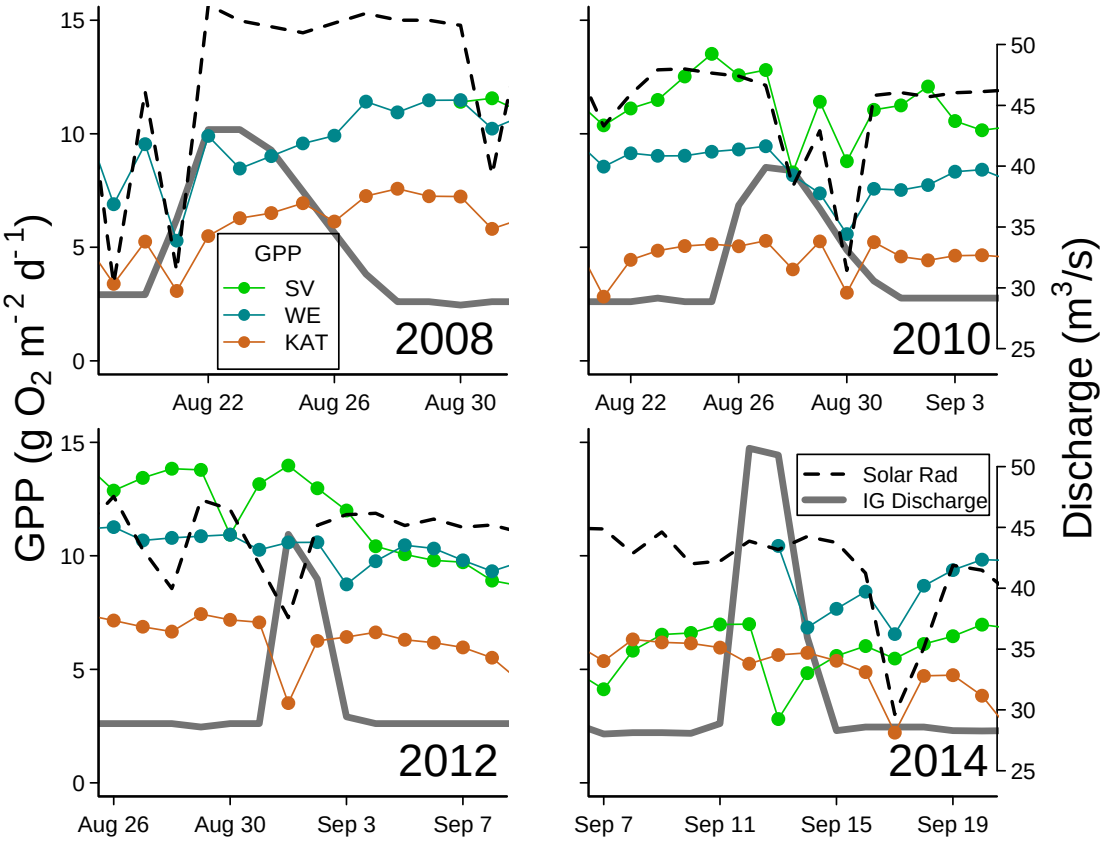

Figure 22. GPP, solar radiation, and Iron Gate discharge for three Klamath River stations during the late summer flow increases from Iron Gate Dam in 2008, 2010, 2012, and 2014. Lines with points are GPP, grey line is discharge below Iron Gate Dam, and dotted line is average daily solar radiation.

4 DISCUSSION

4.1 KLAMATH RIVER PRODUCTIVITY

High rates of GPP, coupled with moderate rates of ER, caused the Lower Klamath River to be mostly autotrophic above the confluence with the Trinity River. Maximum rates of GPP at Seiad (~22 g O m^2 d^{-1}) were among the highest rates of GPP ever reported for streams and rivers. Other river reaches with comparable rates of GPP were tail-water reaches where impoundments stabilized flows and promoted high water clarity such as the Humboldt River in Nevada and the Henry's Fork of the Snake River in Idaho (Davis et al. 2012, Hall et al. 2015b). Some spring fed streams also had comparably high rates of GPP, due to stable flows, high water clarity, and high nutrient concentrations (Acuña et al. 2010, Cohen et al. 2013). The Klamath River may be unique as a highly productive river in that the water is not exceptionally clear (mean summer light attenuation in 2012 = 0.79 m^{-1}; L. Genzoli, unpublished data).

Rates of ER were moderate in the Klamath River compared to other streams and rivers. The 50th quantile of ER for all sites and years on the Klamath River was -5.6 g O m^2 d^{-1}, which is comparable to the 50th quantile of ER estimates for 378 measurements of ER for streams and rivers in the published literature (-5.1 g O m^2 d^{-1}, Hall et al. 2015b). The Klamath River did not experience high rates in ER during the six-month study period, with the 95th quantile of ER for all sites was 11.8 g O m^2 d^{-1}, compared to 18.7 g O m^2 d^{-1} for other streams and rivers.

Although many streams are heterotrophic (higher daily rates of ER than GPP), autotrophic conditions may be common in larger rivers, as they were in the Klamath River. Most studies of ecosystem metabolism have been conducted on smaller streams, and although these streams experienced autotrophic days, they were overall strongly heterotrophic (Roberts et al. 2007, Beauleiu et al. 2013, Roley et al. 2014). Studies in larger rivers have been mixed, with some rivers having heterotrophic conditions and others were balanced or slightly autotrophic with NEP ~0 (Uehlinger et al. 2003, Hall et al. 2015b). Time series of metabolism in larger rivers have also shown seasonal trends, with autotrophy important seasonally (Uehlinger 2000, Dodds et al. 2013). Very few studies have reported estimates for NEP as high as the seasonal means for the Klamath. A meta-analysis of 374 estimates of NEP only reported 3% of measurements with NEP as high or higher than seasonal averages at Seiad and Weitchpec, where NEP was ~2.5 g O m^2 d^{-1} during the six month study period, and NEP was slightly higher (~0.1 g O m^2 d^{-1}) when considering the summer-only data. Mean NEP at Turwar was -0.2 g O m^2 d^{-1} for the whole season and summer only months, putting Turwar at the 87th quantile of NEP estimates from this meta-analysis (Hall et al. 2015b). The prevalence of autotrophic conditions in the Klamath River suggests that in-stream processes drive the riverine food-web.

4.2 ROLE OF DISCHARGE IN SUMMER METABOLISM

Mean summer base-flow was significantly related to mean summer GPP and ER at two of the three study sites (Figure 14). At Weitchpec and Turwar, mean summer GPP and ER decreased as mean summer discharge increased among years. Slopes were similar (though inverse) for GPP and ER within these sites due to summer average ER rates reflecting summer average GPP rates at both sites. ER rates similar to GPP rates occured on daily and seasonal time scales,

likely because a large portion of ER in the Klamath was due to macrophytes and algae, along with organisms that are tightly coupled to macrophyte and algal production.

Mean summer base-flow rates could influence metabolism rates though several mechanisms. Mean depth increases with increasing discharge, which can decrease light available to the benthos in parts of the riverbed, thereby lowering photosynthetic potential and GPP at the reach scale (Vadeboncoeur et al. 2008). In the Lower Klamath River, lower base-flow results in increased nutrients, due to less tributary dilution of nutrients from upstream sources (Asarian and Kann 2010). Increased water temperatures, which were correlated with base-flow on the scale of summer averages, are often associated with increased rates of GPP and ER and may promote higher rate of metabolism on the Klamath River (Demars et al. 2011, Hall et al. 2015a).

Means of summer ecosystem metabolism at Seiad did not follow the same patterns as at Weitchpec and Turwar (Figure 14). With the exception of 2011, which was a high water year, base-flows ranged from approximately 30 to 36 m^3/s, compared to a 100% increase in base-flow at the other two sites. The ~20% increase in base-flow at Seiad may not be enough variation in base-flow discharge to affect rates of metabolism or to detect a relationship. The relationship between mean summer ER and base-flow at Seiad was not statistically significant, but ER generally decreased with increasing base-flow as it did at Weitchpec and Turwar.

Antecedent conditions may influence summer rates of GPP and ER. At Seiad, there was a general decrease among years in summer average GPP and ER as the size of the largest winter flood increased, but the relationship was not significant for either metabolism metric (Figure 16). Winter floods could be influential on rates of metabolism the following summer by washing out the established macrophyte and algal community. Higher flows have greater water velocity, which can scour periphyton (Peterson and Stevenson 1992, Peterson 1996), reducing the biomass available to generate GPP. In the Klamath River, flow is the strongest predictor of periphyton biomass and the seasonal succession of periphyton species composition (Asarian et al. 2015). In a study of a gravel bed river in Switzerland, Uehlinger (2000) found that daily GPP and ER could be predicted in part by the time since that last bed-moving flow event. Other flood metrics may better explain GPP in the Klamath River, such as time since last flood or number of winter floods.

4.3 ROLE OF LIGHT AND PROPORTION OF DISCHARGE FROM IRON GATE DAM ON DAILY VARIATION IN GPP

Daily variation in GPP was positively related to the fraction of discharge from Iron Gate Dam and light within sites. Maximum values of GPP occurred during times of high light and high fraction of Iron Gate discharge (Figure 20). The Upper Klamath Basin (i.e., upstream of Iron Gate Dam) is the major source of nutrients to the lower river, with dilution from tributaries and seasonal uptake by periphyton reducing nutrient concentrations downstream from the dam (Asarian and Kann 2010). Therefore, when the fraction of discharge from Iron Gate was low, nutrient concentrations were also low, and when the fraction of discharge from Iron Gate was high, nutrient concentrations were high (Figure 21). The time series models predicted increases in GPP from ~2 to ~9 g O_2 m^{-2} d^{-1} at sites from these low to high nutrient conditions.

Increased depths associated with higher flows (which occurred when the fraction of discharge from Iron Gate was low) could reduce rates of GPP. Increased discharge has been associated with reduced rates of GPP in the Chattahoochee River, where decreases in depth leading to increased light at the benthic zone was cited as a plausible explanation for the higher rates of GPP (Dodds et al. 2013). Increases in river flow increase mean depth, which likely limits production in the deep pools, but also widens the river and opens up new shallow areas for algae to colonize. The effects of reduced benthic light may be felt most strongly upstream due to faster light attenuation at Seiad (0.96 m^{-1}), or the effects of water clarity may be mitigating by the changing geomorphology, where deeper pool become more prevalent downstream as water becomes more clear.

Light was a major control on GPP in the Klamath River. The time series models predicted that GPP would increase ~3, ~9, and ~1 g O_2 m^{-2} d^{-1} at Seiad, Weitchpec, and Turwar respectively with changes in light associated with day length during the summer (Figure 20). The change in GPP due to day length was similar at Seiad and Turwar relative to their rates of GPP (summer mean 11 and 5 g O_2 m^{-2} d^{-1}, respectively). The change at Weitchpec was three-fold that of Seiad, likely due to shading from canyon walls that exaggerate the effects of changing solar angles associated with shorter days (Yard et al. 2005).

Incorporating measured light into the model, which reflects daily cloud cover (and likely smoke from wildfires), improved the model's ability to predict GPP (Figure 19). Light is often identified as a primary control on stream GPP, with factors that control light at the benthos being important predictors of GPP (Roberts 2007, Beaulieu et al. 2013, Hall et al. 2015a). In addition to cloud cover, which is represented in the light senor data, riparian shading, shading from canyon walls, and increased water-column turbidity can decrease light to riverine primary producers (Dodds et al. 2013, Ochs et al. 2013, Hall et al. 2015a). Although applying data from one sensor to all sites would capture low light events attributed to weather that affects a large region, sensors able to detects sub-regional weather and smoke would better predict GPP on the Klamath River. In the absence of additional sensors, using satellite-derived datasets such as the North American Land Data Assimilation System[4] (NLDAS, Xia et al. 2012) may be an improvement on the day-length only light model. Including turbidity data as a predictor of daily GPP may future improve the models ability to predict GPP because turbidity influence the amount of light reaching the benthos.

4.4 RESERVOIR ALGAL BLOOM EFFECT ON WHOLE RIVER METABOLISM AND MINIMUM DISSOLVED O_2

The algal bloom generally lowered GPP in the Klamath River, with the largest reduction at Seiad, and effects diminishing at downstream sites. Although increased water-column phytoplankton from reservoirs increase production in the water column, the decrease in water clarity reduces light availability to the benthos, reducing rates of production from benthic algae (Genzoli 2013, Genzoli and Hall, in review). Using the time series model, which explains daily rates of GPP and takes multiple variables into account, we predicted that GPP at Seiad would be ~3.5 g O m^2 d^{-1} lower during the bloom than before the bloom, given similar light and nutrient

[4] Time series available at: http://disc.sci.gsfc.nasa.gov/hydrology/data-rods-time-series-data

conditions. The decrease in predicted GPP at Weitchpec was < 2 g O m^2 d^{-1}, and the decrease at Turwar was < 0.2 g O m^2 d^{-1}. The decreased effect of the bloom on GPP at down-river sites is expected because concentrations of cyanobacteria generally decreased in a downstream direction (Appendix A).

More traditional statistical tests of the effects of the reservoir algal bloom on ecosystem metabolism produced mixed results. Comparison of mean rates of summer GPP between bloom and non-bloom conditions generally supported the results of the time series model, which indicated an effect of the bloom that was strongest up river and very week near the river's mouth. At Seiad, mean GPP in the summer prior to the algal bloom was higher than during the bloom in all years, and the paired t-test of the summer means indicated a statistically significant decline in GPP from non-bloom to bloom conditions (Table 5). At Weitchpec, there was a decrease in mean GPP from non-bloom to bloom conditions in all years, except for 2011 where high flows into July likely suppressed GPP until later in the season when the bloom was affecting the river, but the decrease in GPP was not statistically significant. At Turwar, GPP decreased some years and increased others. Summer means of ER, and NEP by year before and during algal blooms revealed no significant changes in ecosystem metabolism. Although we would expect river ER to increase with a bloom which carries organic material into the river and which blocked light to the benthic zone, ER also follows GPP, which generally decreased at sites during the bloom (Figure 8). At Seiad, ER decreased across years with the onset of the bloom, whereas there was a slight increase in ER at Weitchpec, and no change at Turwar. These shifts in ER relative to GPP drove the river toward heterotrophy (lower NEP) at Seiad and Weitchpec, and had minimal effects at Turwar. Light, nutrient, and temperature conditions also change seasonally, so changes in ecosystem metabolism that happen with the bloom should be interpreted cautiously, as other factors are also acting on rates production and respiration.

Daily minimum dissolved O_2 saturation decreased with increasing GPP, with lower minimum dissolved O_2 saturation per unit of GPP during bloom conditions than during non-bloom conditions (Figure 12). GPP controled minimum dissolved O_2 saturation via close coupling with ER. On the Klamath River in the summer months ER reflected rates of GPP because river autotrophs respire, as well as support heterotrophs that are closely associated with autotrophic production (Hall and Beaulieu 2013). Few inputs of terrestrial material occur due to minimal precipitation events in the summer, and upstream dams likely cut off the flow of organic materials from upstream (Ulseth and Hall 2015), reducing ER events that are not coupled with GPP. Daily minimum dissolved O_2 saturation was lowest when GPP was highest, because high dissolved O_2 during the day resulted in low dissolved O_2 at night. At Seiad and Weitchpec, NEP, was lower during bloom than during non-bloom conditions (more ER per unit of GPP). This reduction in NEP could occur if increased shading of benthic algae occurred due to turbidity from the bloom, while the algal community continued to respire even though their photosynthetic ability was reduced.

The timing and magnitude of the algal bloom are difficult to quantify, in part due to the complex nature of blooms on the river. Although the river often appeared to shift from non-bloom to bloom conditions in the late summer, real-time estimates of cyanobacteria concentrations from the sondes show highly variable cyanobacteria concentrations during bloom periods, likely driven by heterogeneity in Iron Gate Reservoir where bloom conditions near the reservoir outflow can change rapidly due to wind and algal buoyancy. Comparing river metabolism

metrics to daily cyanobacteria concentrations could be an alternative method to quantify the effects of cyanobacteria, but the daily data from the sensors are not always representative of the whole river reach. Cyanobacteria concentrations generally decreased in a downstream direction from the reservoirs, so we would expect to see similar patterns in bloom pulses at all sites. In some years, the cyanobacteria probes did not record data at all sites, or daily patterns in cell density was not consistent among sites, necessitating generalization of bloom conditions over a season rather than on a day-by-day basis.

4.5 CONCLUSIONS

The Klamath River was highly productive. Rates of GPP in the Klamath River controlled dissolved O_2 minima due to the tight coupling of ER with GPP, with dissolved O_2 saturation dipping below water quality goals at high rates of GPP. At times, rates of GPP in the Klamath were among the highest measured in streams and rivers. High rates of GPP paired with moderate rates of ER resulted in mostly autotrophic conditions in the Klamath River above the confluence with the Trinity River, and an NEP of ~0 at Turwar. Positive NEP is not commonly reported in streams and rivers, but would be expected in a highly productive river.

Summer mean GPP was related to discharge metrics. Summer mean GPP was low during years of high summer base-flow and GPP was high in dryer years at Weitchpec and Turwar. Although mean summer GPP at Seiad was not correlated with summer base-flow, the timing or size of floods may have influenced rates of summer GPP. Mean summer GPP at Seiad was negatively related to the size of the largest flood the previous year. Floods scour benthic habitat, resetting periphyton and macrophyte growth, so the timing and size of floods could influence the rates of GPP, even months after their occurrence. Summer base-flow discharge may affect GPP due to changes in width, depth, and river velocity, as well through secondary control of other variables, including nutrient concentrations and water temperature.

Light and nutrients likely controlled daily variation in GPP within a season on the Klamath River. Nutrient concentrations increased as the fraction of discharge from Iron Gate increased, and this discharge metric was positively related to rates of GPP across all sites and years. Within a season, lower ambient light conditions resulted in lower rates of GPP. Additional environmental variables that influence light conditions at the riverbed are likely important to controlling rates of GPP.

The algal bloom, which reduces light to the benthos, reduced rates of GPP in the Klamath River, with stronger effects upstream than downstream. The relationship between GPP and dissolved O_2 minima also shifted during the bloom, so that decreased GPP did not result in increased dissolved O_2 minima.

Identification of the controls on GPP, especially in the summer months when water quality is compromised, can inform targeted management actions. Further understanding the specific mechanisms limiting production at the ecosystem level may require additional data collection including ambient light conditions representative of the light at the river surface, measurements of water clarity, and high frequency measurements of nutrient concentrations and loads. Understanding how other water quality parameters such as pH and algal biomass relate to GPP may provide guidance in setting target rates of GPP in the Klamath River.

5 REFERENCES CITED

Acuña, V., C. Vilches, and A. Giorgi. 2010. As productive and slow as a stream can be-the metabolism of a Pampean stream. Journal of the North American Benthological Society, 30:71-83.

Asarian, E., J. Kann, and W. Walker. 2010. Klamath River Nutrient Loading and Retention Dynamics in Free-Flowing Reaches, 2005-2008. Final Technical Report to the Yurok Tribe Environmental Program, Klamath, CA. 59pp + appendices. http://www.riverbendsci.com/reports-and-publications-1/Klamath0508_nutrient_dynamics_final_report_revised.pdf

Asarian, E. and J. Kann. 2013. Synthesis of Continuous Water Quality Data for the Lower and Middle Klamath River, 2001-2011. Prepared by Kier Associates and Aquatic Ecosystem Sciences for the Klamath Basin Tribal Water Quality Work Group. 50p. + appendices. http://www.riverbendsci.com/reports-and-publications-1/Klamath_2001_2011_sonde_rpt_20130502_final.pdf

Asarian, J.E., Y. Pan, N.D. Gillett, and J. Kann. 2015. Periphyton Assemblages and Associated Environmental Conditions in the Klamath River 2004-2013. Prepared by Riverbend Sciences, Portland State University, and Aquatic Ecosystem Sciences LLC. for the Klamath Basin Tribal Water Quality Group. 48p. + appendices. http://googledrive.com/host/0B2p7GuVSL4OXYjZIbmRDUjgyd2M/KlamPeriphyton_Phase2_20150819final.pdf

Beaulieu, J.J., C.P. Arango, D. A. Balz, and W. D. Shuster. 2013. Continuous monitoring reveals multiple controls on ecosystem metabolism in a suburban stream. Freshwater Biology 58:918-937.

Chapra, S. C., and D. M. Di Toro. 1991. Delta method for estimating primary production, respiration, and reaeration in streams. Journal of Environmental Engineering 117: 640-655.

Cross, W. F., C.V. Baxter, E. J. Rosi-Marshall, R.O. Hall, T. A. Kennedy, K. C. Donner, H. A. Wellard-Kelly, S. E. Seegert, K. E. Behn, and M. D. Yard. 2013. Food-web dynamics in a large river discontinuum. Ecological Monographs 83:311-337.

Clark, J. S. 2007. *Models for ecological data: an introduction*. Princeton, New Jersey, USA: Princeton University Press.

Cohen, M. J., M. J. Kurz, J. B. Heffernan, J. B. Martin, R. L. Douglass, C. R. Foster, and R. G. Thomas. 2013. Diel phosphorus variation and the stoichiometry of ecosystem metabolism in a large spring-fed river. Ecological Monographs, 83:155-176.

Davis, C. J., C. H. Fritsen, E. D. Wirthlin, and J. C. Memmott. 2012. High rates of primary productivity in a semi-arid tailwater: implications for self- regulated production. River Research and Applications 28:1820–1829.

Demars, B. O., M. J. Russell, J. S. Olafsson, G. M. Gislason, R. Gudmundsdottír, G. Woodward, J. Reiss, D. E. Pichler, J. J. Rasmussen, and N. Friberg. 2011. Temperature and the metabolic balance of streams. Freshwater Biology, 56:1106-1121.

Dodds, W. K. 2006. Eutrophication and trophic state in rivers and streams. Limnology and Oceanography 51:671-680.

Dodds, W. K., A. M. Veach, C. M. Ruffing, D. M. Larson, J. L. Fischer, and K. H. Costigan. 2013. Abiotic controls and temporal variability of river metabolism: multiyear analyses of Mississippi and Chattahoochee River data. Freshwater Science, 32:1073-1087.

Fellows, C.S., J.E. Clapcott, J.W. Udy, S. E. Bunn, B.D. Harch, M.J. Smith, and P.M. Davies. 2006. Benthic Metabolism as an Indicator of Stream Ecosystem Health. Hydrobiologia 572:71-87.

Garcia, H. E., and L. I. Gordon. 1992. Oxygen solubility in seawater: Better fitting equations. Limnology and oceanography, 37:1307-1312.

Gelman, A., and J. Hill. 2007. *Data analysis using regression and multilevel/hierarchical models*. Cambridge University Press.

Genzoli, L. 2013. Shifts in Klamath River metabolism following cyanobacterial bloom. MS thesis. University of Wyoming, Laramie, Wyoming. 53 p.

Genzoli, L. and R. O. Hall. In review. Shifts in Klamath River metabolism following a reservoir cyanobacterial bloom.

Hall, R. O., T. A. Kennedy, and E. J. Rosi-Marshall. 2012. Air-water oxygen exchange in a large whitewater river. Limnology & Oceanography: Fluids & Environments 2:1-11.

Hall, R. O., C. B. Yackulic, T. A. Kennedy, M. D. Yard, E. J. Rosi- Marshall, N. Voichick and K.E. Behn. 2015a. Turbidity, light, temperature, and hydropeaking control primary productivity in the Colorado River, Grand Canyon. Limnology and Oceanography, 60: 512-526.

Hall, R. O., J. L. Tank, M. A. Baker, E. J. Rosi-Marshall, and E.R. Hotchkiss. 2015b. Metabolism, Gas Exchange, and Carbon Spiraling in Rivers. Ecosystems, 1-14. DOI: 10.1007/s10021-015-9918-1

Helsel, D.R. and R.M. Hirsch, 2002. Statistical Methods in Water Resources. Techniques of Water Resources Investigations, Book 4, Chapter A3. U.S. Geological Survey, 522p. http://pubs.er.usgs.gov/publication/twri04A3

Holmquist-Johnson, C.L., and R. T. Milhous. 2010. Channel maintenance and flushing flows for the Klamath River below Iron Gate Dam, California: U.S. Geological Survey Open File Report 2010-1086, 31 p

Hornberger, G. M., and M. G. Kelly. 1974. A new method for estimating productivity in standing waters using free oxygen measurements. Journal of the American Water Resources Association 10:265-271.

Jähne, B., and H. Haußecker. 1998. Air-water gas exchange. Annual Review of Fluid Mechanics 30: 443–468.

Karuk Tribe. 2008. Water Quality Assessment Report 2008. Karuk Tribe Department of Natural Resources, Orleans, CA. 75 p. <http://www.klamathwaterquality.com/documents/2009/2008_WQReport_Karuk.pdf> Accessed 2009 21 December.

Karuk Tribe of California. 2010. Water Quality Report for the mid-Klamath, Salmon, Scott, and Shasta Rivers: May-Dec 2009. Karuk Tribe Department of Natural Resources, Orleans, CA. 21 p. <http://www.klamathwaterquality.com/documents/Karuk_2010_WQ_Report_2009.pdf> Accessed 2012 22 October.

Karuk Tribe of California. 2011. Water Quality Assessment Report 2010, Klamath River, Salmon River, Scott River, Shasta River, and Bluff Creek. Karuk Tribe Department of Natural Resources, Orleans, CA. 23 p. <http://www.klamathwaterquality.com/documents/Karuk_2011_WQ_Report_2010.pdf> Accessed 2012 22 October.

Karuk Tribe of California. 2012. Water Quality Assessment Report 2011. Klamath River, Salmon River, Scott River, Shasta River, and Bluff Creek. Karuk Tribe Department of Natural Resources, Orleans, CA. 27 p. <http://www.karuk.us/karuk2/images/docs/wqdocuments/2011WQAR.pdf> Accessed 2012 22 October

Karuk Tribe of California. 2013. Water Quality Assessment Report 2013. Karuk Tribe Department of Natural Resources, Orleans, CA. 33 p.

Marcarelli, A. M., C. V. Baxter, M. M. Mineau, and R. O. Hall. 2011. Quantity and quality: unifying food web and ecosystem perspectives on the role of resource subsidies in freshwaters. Ecology 92:1215-1225.

Nimick DA, Gammons CH, Parker SR. 2011. Diel biogeochemical processes and their effect on the aqueous chemistry of streams: A review. Chemical Geology 283:3–17.

North Coast Regional Water Quality Control Board (NCRWQCB). 2010. Final Staff Report for the Klamath River Total Maximum Daily Loads (TMDLs) Addressing Temperature, Dissolved Oxygen, Nutrient and Microcystin Impairments in California, the Proposed Site Specific Dissolved Oxygen Objectives for the Klamath River and California, and the Klamath River and Lost River Implementation Plans. NCRWQCB, Santa Rosa, CA.

Ochs, C. A., O. Pongruktham, and P. V. Zimba. 2013. Darkness at the break of noon: Phytoplankton production in the Lower Mississippi River. Limnology and Oceanography, 58:555-568.

Oliver, A. A., R. A. Dahlgren, and M. L. Deas. 2014. The upside-down river: Reservoirs, algal blooms, and tributaries affect temporal and spatial patterns in nitrogen and phosphorus in the Klamath River, USA. Journal of Hydrology, 519:164-176.

Oregon Department of Environmental Quality (ODEQ). 2010. Upper Klamath and Lost River subbasins; total maximum daily load (TMDL) and water quality management plan (WQMP). Oregon Department of Environmental Quality, Portland, OR. Available online at http://www.deq.state.or.us/WQ/TMDLs/klamath.htm

Palmer, M., and C. Febria. 2012. The heartbeat of ecosystems. Science 336:1393-1394.

Peterson, C. G. 1996. Response of benthic algal communities to natural physical disturbance. In R. J. Stevenson, M. L. Bothwell, and R. L. Lowe (eds.) Algal ecology: freshwater benthic ecosystems, Academic Press, San Diego, CA, USA: 375-402.

Peterson, C. G. and R. J. Stevenson. 1992. Resistance and resilience of lotic algal communities - importance of disturbance timing and current. Ecology 73 (4): 1445-1461.

Roberts, B. J., P. J. Mulholland, and W. R. Hill. 2007. Multiple scales of temporal variability in ecosystem metabolism rates: results from 2 years of continuous monitoring in a forested headwater stream. Ecosystems 10:588-606.

Roley, S. S., J.L. Tank, N. A. Griffiths, R. O. Hall, and R. T. Davis. 2014. The Influence of Floodplain Restoration on Whole-Stream Metabolism in an Agricultural Stream: Insights from a 5-year Continuous Data Set. Freshwater Science, 33:1043-1059.

Thorp, J. H., and M. D. Delong. 2002. Dominance of autochthonous autotrophic carbon in food webs of heterotrophic rivers. Oikos 96:543-550.

Uehlinger, U. 2000. Resistance and resilience of ecosystem metabolism in a flood- prone river system. Freshwater Biology 45:319–332.

Uehlinger, U., B. Kawecka, and C. T. Robinson. 2003. Effects of experimental floods on periphyton and stream metabolism below a high dam in the Swiss Alps (River Spöl). Aquatic Sciences, 65:199-209.

Ulseth, A. J., and R.O. Hall. 2015. Dam tailwaters compound the effects of reservoirs on the longitudinal transport of organic carbon in an arid river. Biogeosciences Discussions, 12:8.

Van de Bogert, M. C., S. R. Carpenter, J. J. Cole, and M. L. Pace. 2007. Assessing pelagic and benthic metabolism using free water measurements. Limnology and Oceanography: Methods 5:145–155.

Vadeboncoeur, Y., G. Peterson, M.J. Vander Zanden, J. Kalff. 2008. Benthic algal production across lake size gradients: interactions among morphometry, nutrients, and light. Ecology 89:2542–52.

Woodward, G., M. O. Gessner, P. S. Giller, V. Gulis, S. Hladyz, A. Lecerf, B. Malmqvist, B. G. McKie, S. D. Tiegs, H. Cariss, M. Dobson, A. Elosegi, V. Ferreira, M. A. Graca, T.

Fleituch, J. O. Lacoursiere, M. Nistorescu, J. Pozo, G. Risnoveanu, M. Schindler, A. Vadineanu, L. B. Vought, and E. Chauvet. 2012. Continental-scale effects of nutrient pollution on stream ecosystem functioning. Science, 336:1438-1440.

Xia, Y., K. Mitchell, M. Ek, J. Sheffield, B. Cosgrove, E. Wood, L. Luo, C. Alonge, H. Wei, J. Meng, B. Livneh, D. Lettenmaier, V. Koren, Q. Duan, K. Mo, Y. Fan, and D. Mocko, 2012. Continental-Scale Water and Energy Flux Analysis and Validation for the North American Land Data Assimilation System Project Phase 2 (NLDAS-2): 1. Intercomparison and Application of Model Products. Journal of Geophysical Research: Atmospheres 117:D03109. doi: 10.1029/2011JD016048.

Yard, M. D., G. E. Bennett, S. N. Mietz, L. G. Coggins Jr, L. E. Stevens, S. Hueftle, and D. W. Blinn. 2005. Influence of topographic complexity on solar insolation estimates for the Colorado River, Grand Canyon, AZ. Ecological Modelling 183:157–172.

Young, R.G., C. D. Matthaei, and C. R. Townsend. 2008. Organic matter breakdown and ecosystem metabolism: functional indicators for assessing river ecosystem health. Journal of the North American Benthological Society 27:605-625.

Yurok Tribe Environmental Program. 2010. Final 2009 Klamath River Continuous Water Quality Monitoring Summary Report. Prepared by Scott Sinnott. YTEP Water Division, Klamath, CA. 65 p.

Yurok Tribe Environmental Program. 2011. Final 2010 Klamath River Continuous Water Quality Monitoring Summary Report. Prepared by Scott Sinnott. YTEP Water Division, Klamath, CA. 54 p.

Yurok Tribe Environmental Program. 2012. Final 2011 Klamath River Continuous Water Quality Monitoring Summary Report. Prepared by Scott Sinnott. YTEP Water Division, Klamath, CA. 57 p.

Yurok Tribe Environmental Program. 2013. Draft 2012 Klamath River Continuous Water Quality Monitoring Summary Report. Prepared by Matthew Hanington. YTEP Water Division, Klamath, CA. 69 p.

6 ACKNOWLEDGMENTS

The report was prepared for the Klamath Tribal Water Quality Consortium (formerly known as the Klamath Basin Tribal Water Quality Work Group) using funds awarded to the Consortium by the U.S. EPA Region 9 and administered by the Karuk Tribe. The Yurok Tribe and Karuk Tribe contributed data to this report.

APPENDIX A: CYANOBACTERIAL BLOOM TIMING

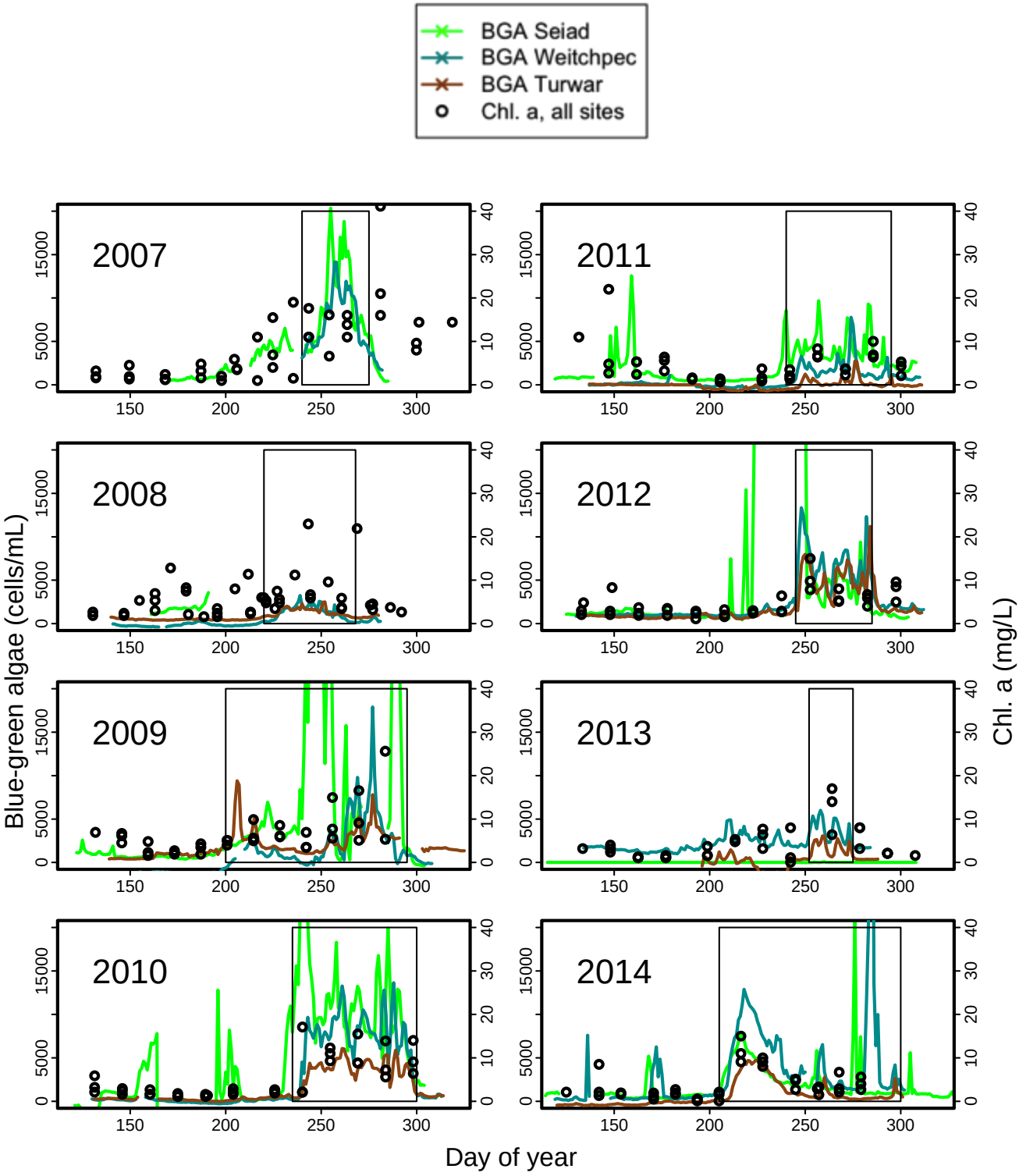

Figure A 1. Lines represent mean daily blue green algae estimates based on sonde phycocyanin sensors at three sites on the Lower Klamath River. Black dots are Chl. a measurements, and black rectangles denote the period that we defined as active algal bloom periods.

APPENDIX B: EXAMPLES OF MODEL FITS FOR METABOLISM ESTIMATES

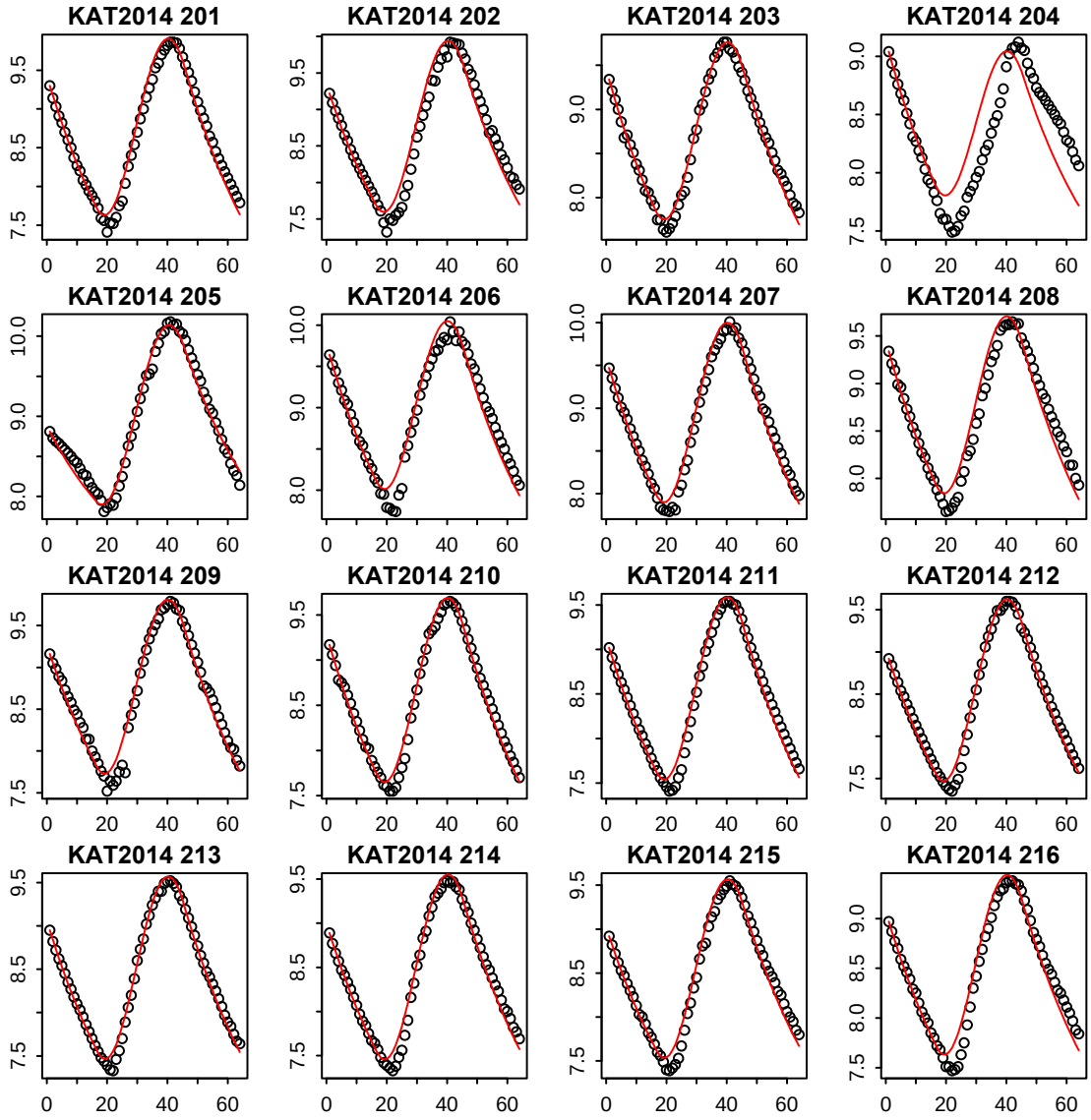

Figure B 1. Examples of model fits used for calculating metabolism metrics for Turwar from 20 July 2014 to 4 August 2014. Black circles are measured dissolved O_2 (g/mL; y axis) over a 32-hour extended day-length period. Red line is the model fit.

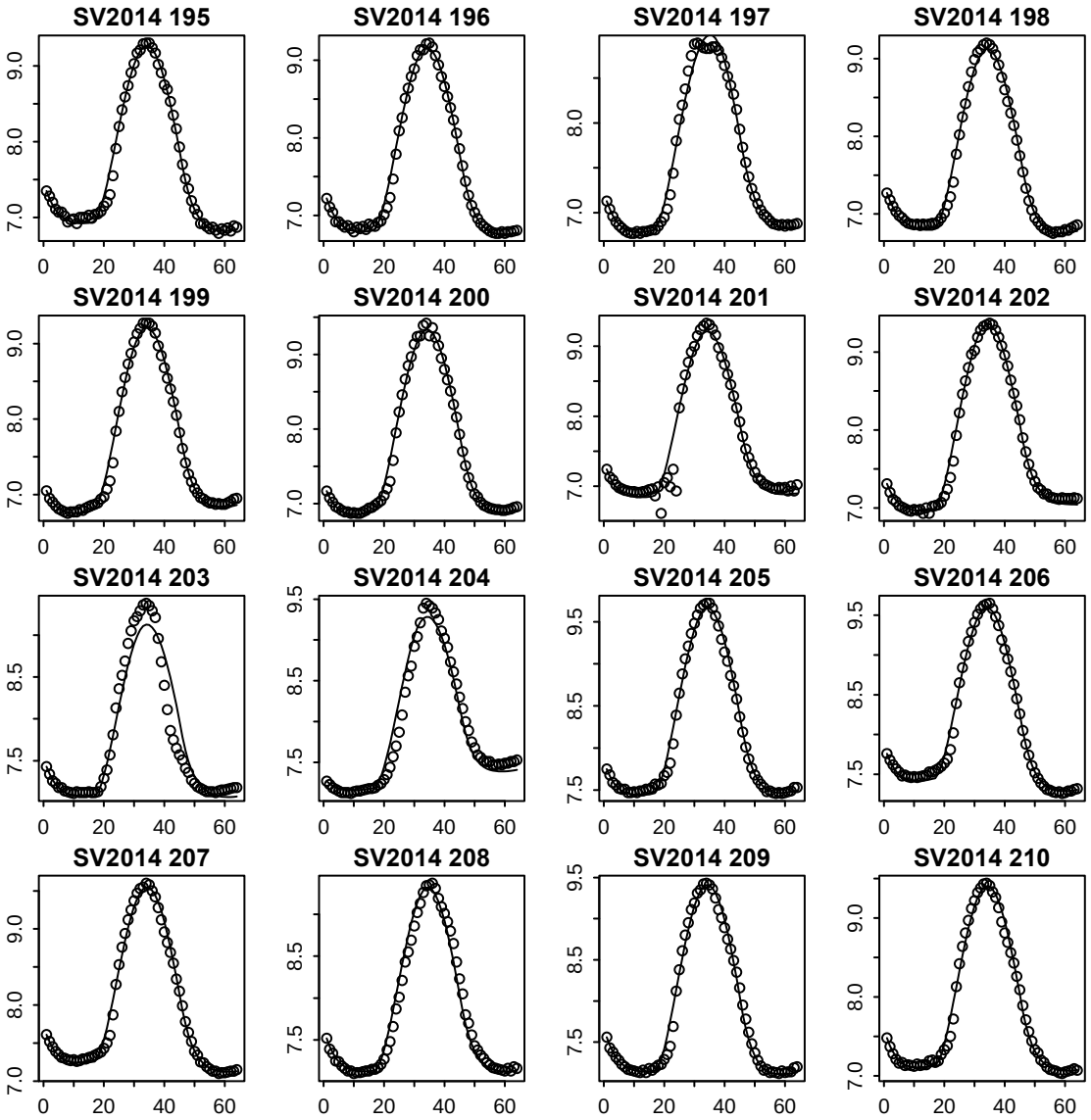

Figure B 2. Examples of model fits used for calculating metabolism metrics for Seiad from 14 July 2014 to 29 July 2014. Black circles are measured dissolved O_2 (g/mL; y axis) over a 32-hour extended day-length period. Black line is the model fit.

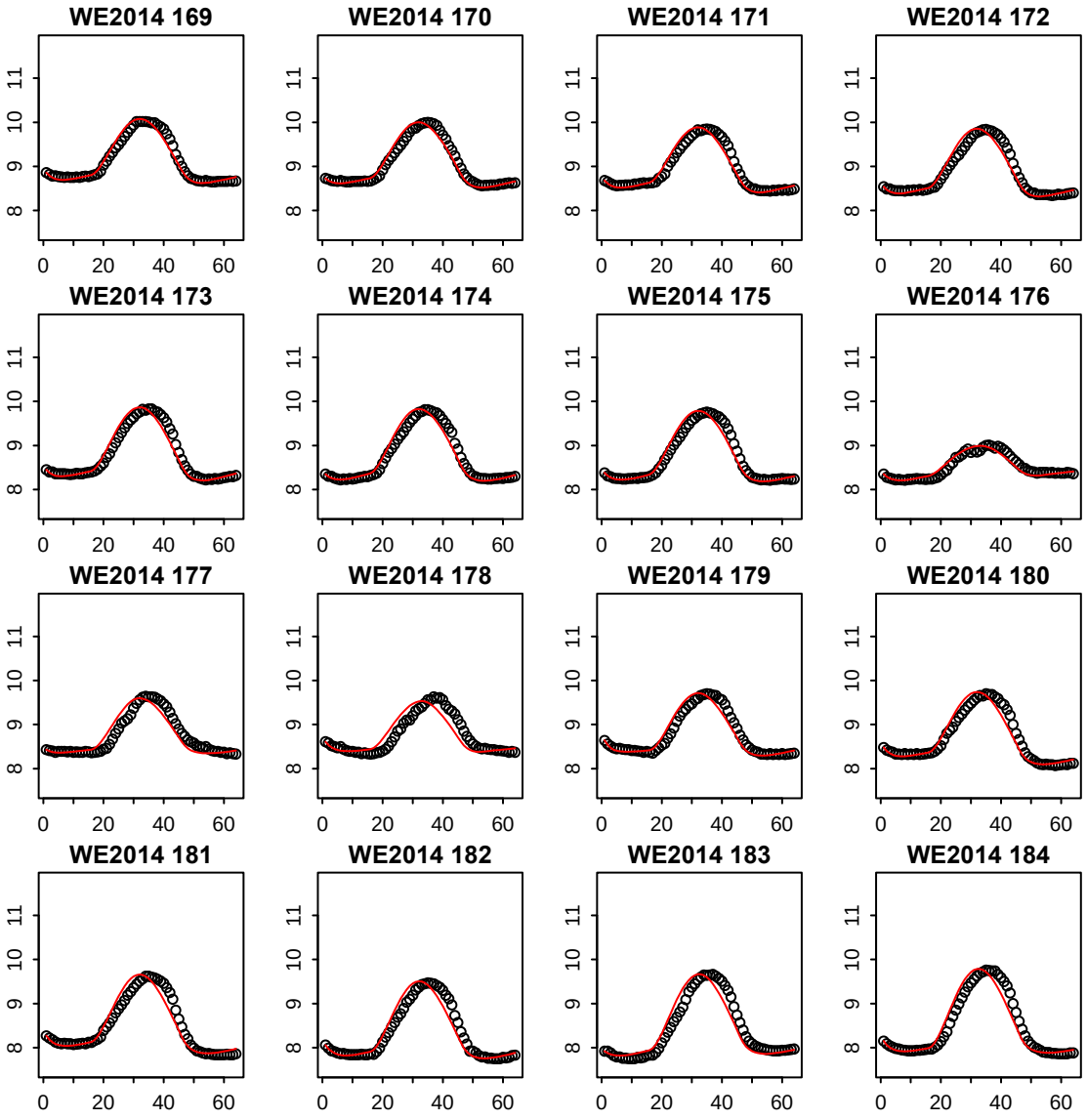

Figure B 3. Examples of model fits used for calculating metabolism metrics for Weitchpec from 18 June 2014 to 3 July 2014. Black circles are measured dissolved O_2 (g/mL; y axis) over a 32-hour extended day-length period. Red line is the model fit.

APPENDIX C: PARAMETER ESTIMATES FOR TIME SERIES MODELS

Table C. 1. Means of the posterior distribution for parameters from the model describing daily GPP at Seiad during the summer months, where $\beta 0$ is the model constant and θ is the auto-correlation term.

Site	Year	$\beta 0$	Bloom Status	Predicted light	Fraction of Q from Iron Gate	θ
Seiad	2007	-0.687	-1.181	0.00205	1.990	0.838
	2008	-0.378	-0.300	0.00479	2.357	0.640
	2009	-0.464	-1.496	0.00725	2.202	0.660
	2010	-0.620	-0.584	0.00384	1.893	0.689
	2011	-0.725	-0.547	0.00093	2.168	0.887
	2012	-0.370	-0.621	0.00078	2.333	0.812
	2013	-0.568	-0.629	0.00038	2.151	0.840
	2014	-0.461	-0.584	0.00426	1.877	0.485
	pooled	-0.515	-0.738	0.00306	2.135	NA
Observation error:		0.098				
Process error:		1.097				

Table C. 2. Means of the posterior distribution for parameters from the model describing daily GPP at Weitchpec during the summer months, where $\beta 0$ is the model constant and θ is the auto-correlation term.

Site	Year	$\beta 0$	Bloom Status	Predicted light	Fraction of Q from Iron Gate	θ
Weitchpec	2007	-5.069	-0.031	0.00662	4.232	0.811
	2008	-2.372	-0.483	0.00350	4.160	0.794
	2009	-0.837	-1.378	0.00646	3.440	0.613
	2010	-2.222	-0.408	0.00259	3.009	0.902
	2011	-3.230	-0.096	0.00299	4.776	0.879
	2012	-3.313	-0.085	0.00388	3.988	0.829
	2013	-8.449	-0.042	0.01635	4.913	0.471
	2014	-9.955	0.810	0.02068	3.681	0.312
	pooled	-3.482	-0.206	0.00785	4.014	NA
Observation error:		0.163				
Process error:		1.066				

Table C. 3. Means of the posterior distribution for parameters from the model describing daily GPP at Weitchpec during the summer months, where $\beta 0$ is the model constant and θ is the auto-correlation term. This model used measured light.

Site	Year	$\beta 0$	Bloom Status	Measured light	Fraction of Q from Iron Gate	θ
Weitchpec	2007	NA	NA	NA	NA	NA
	2008	-1.868	-0.311	0.44879	2.859	0.737
	2009	0.718	-1.571	0.52559	2.449	0.645
	2010	-1.596	-0.308	0.22303	2.483	0.895
	2011	-0.756	-0.359	0.05945	2.912	0.905
	2012	-1.187	-0.379	0.23616	2.797	0.814
	2013	-1.098	-0.760	0.83935	2.452	0.566
	2014	-1.352	-0.415	0.98615	1.741	0.549
	mean	-0.980	-0.586	0.47559	2.538	NA
Observation error:		0.064				
Process error:		0.866				

Table C. 4. Means of the posterior distribution for parameters from the model describing daily GPP at Turwar during the summer months, where $\beta 0$ is the model constant and θ is the auto-correlation term.

Site	Year	$\beta 0$	Bloom Status	Predicted light	Fraction of Q from Iron Gate	θ
Turwar	2007	-0.106	-0.109	0.00079	1.728	0.780
	2008	0.342	0.087	0.00067	2.254	0.682
	2009	0.216	-0.147	0.00145	1.639	0.725
	2010	0.137	-0.034	0.00092	1.645	0.710
	2011	0.104	0.033	0.00026	2.158	0.766
	2012	-0.024	0.009	0.00058	1.455	0.838
	2013	-0.215	-0.156	0.00135	1.532	0.773
	2014	-0.315	-0.147	0.00349	1.213	0.566
	mean	0.046	-0.057	0.00117	1.718	NA
Observation error:		0.113				
Process error:		0.773				

APPENDIX D: MODELED GPP WITH MEASURED GPP AND MODEL PARAMETERS

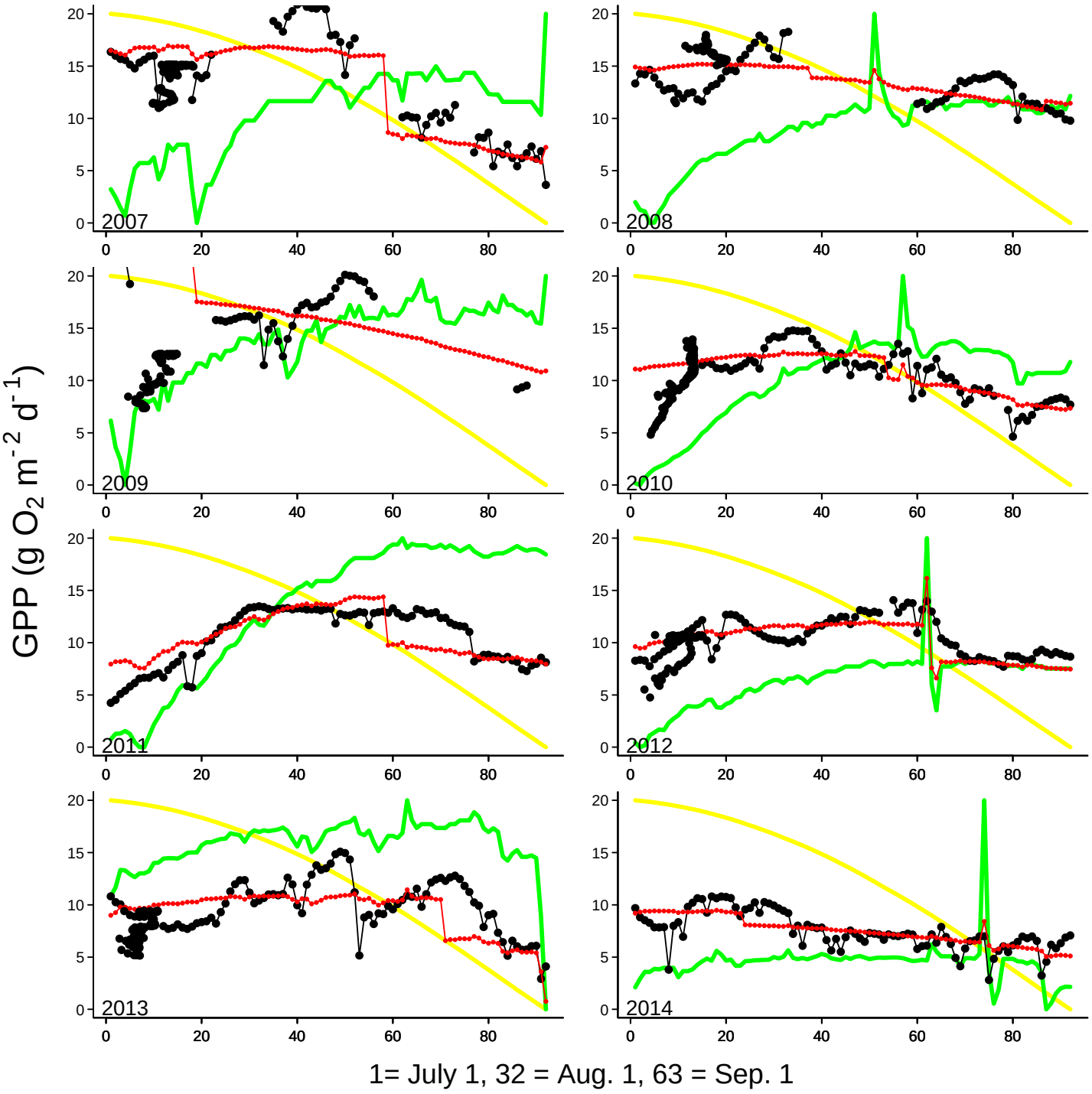

Figure D 1. Modeled GPP for Seiad (red line) with measured GPP (black line) for each of eight study years during July, August, and September. Yellow line is modeled light representing seasonal change in day length and green line represents the fraction of discharge from Iron Gate Dam. Scales for fraction of flow from Iron Gate and light are arbitrary and are used to show trends in these variables.

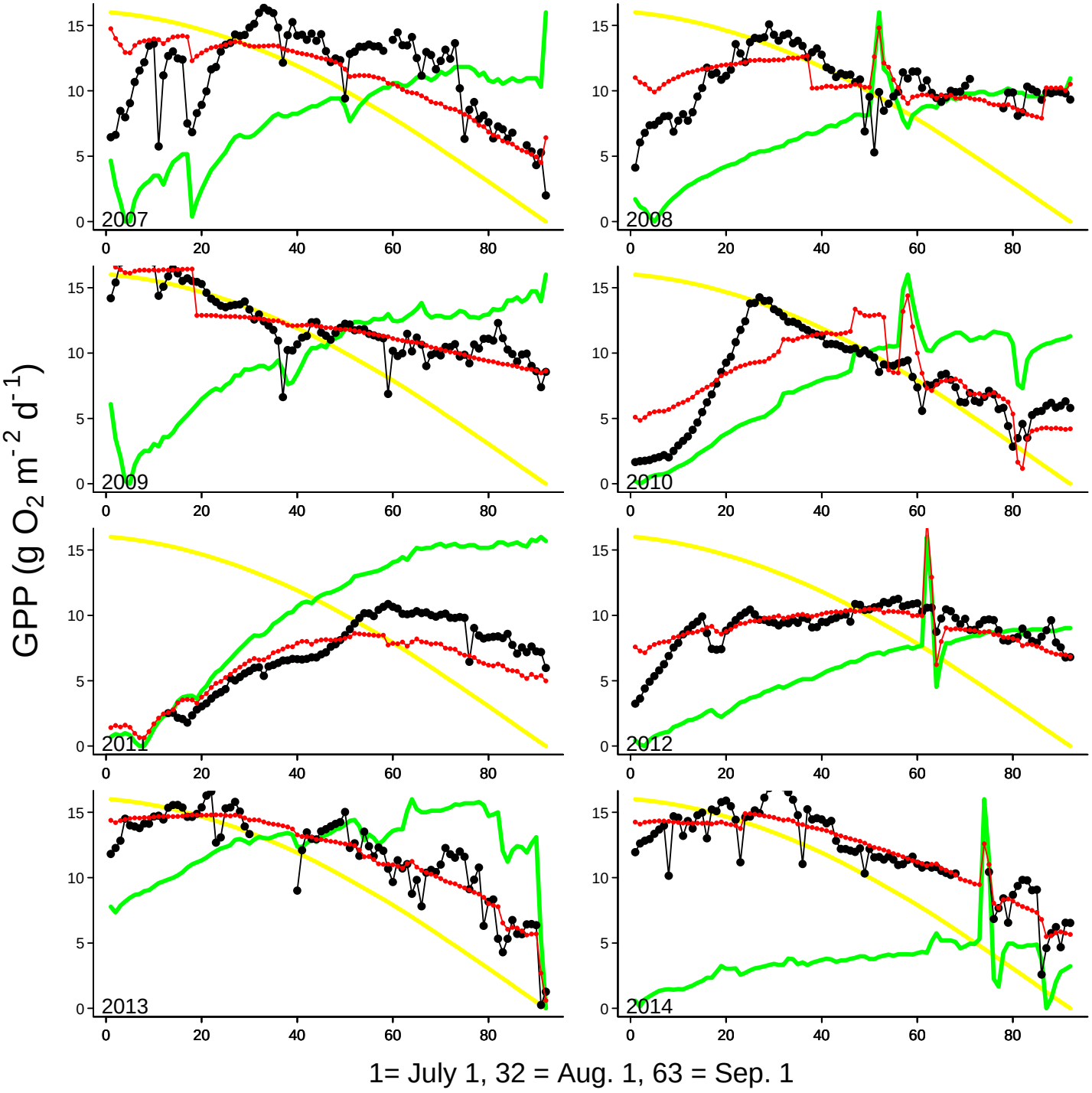

Figure D 2. Modeled GPP for Weitchpec (red line) with measured GPP (black line) for each of eight study years during July, August, and September. Yellow line is modeled light representing seasonal change in day length and green line represents the fraction of discharge from Iron Gate Dam. Scales for fraction of flow from Iron Gate and light are arbitrary and are used to show trends in these variables.

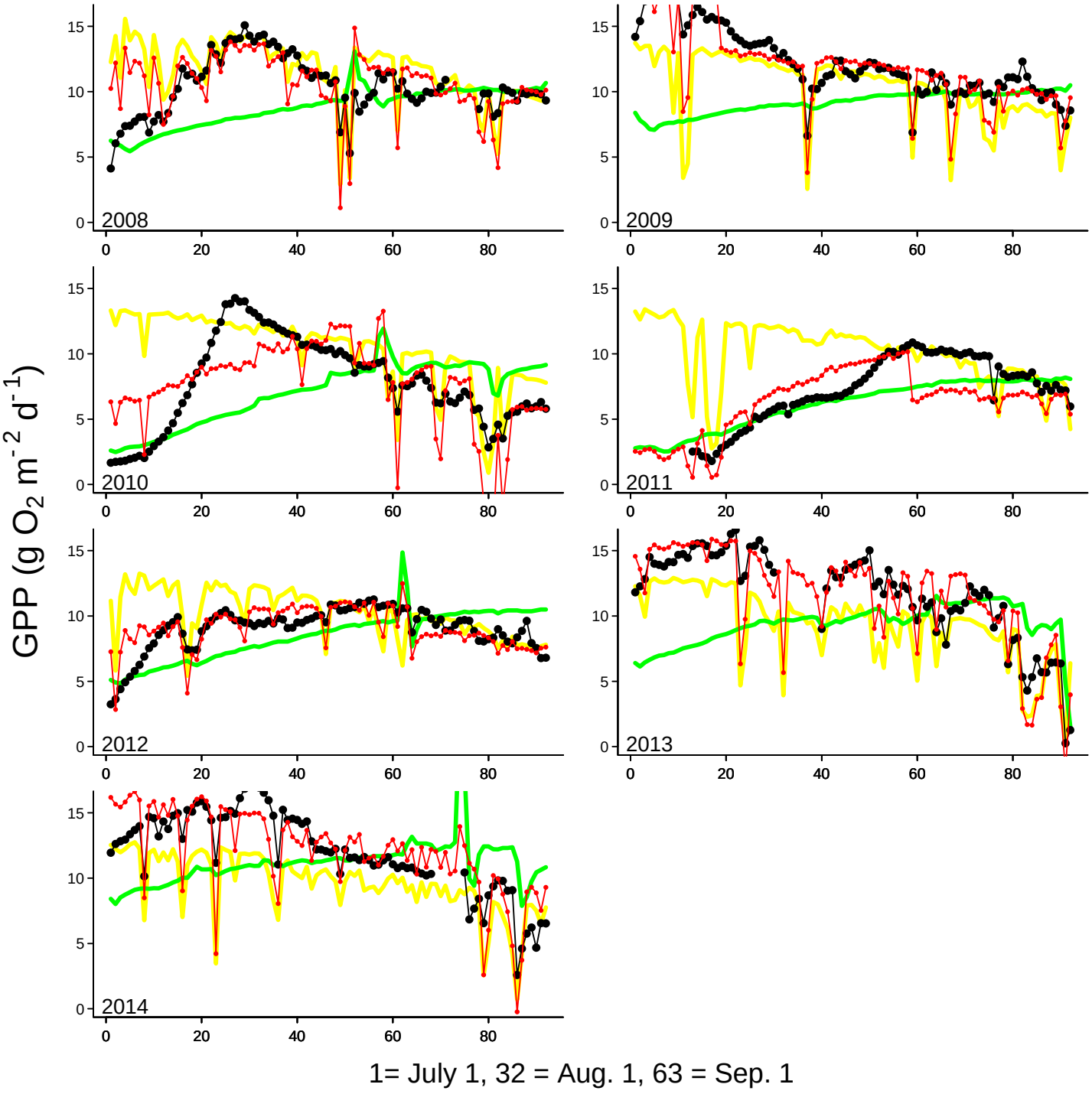

Figure D 3. Modeled GPP for Weitchpec (red line) with measured GPP (black line) for each of seve study years during July, August, and September, when measured solar radiation data was available for Weitchpec. Yellow line is measured solar radiation representing seasonal change in day length and cloud cover and green line represents the fraction of discharge from Iron Gate Dam. Scales for fraction of flow from Iron Gate and light are arbitrary and are used to show trends in these variables.

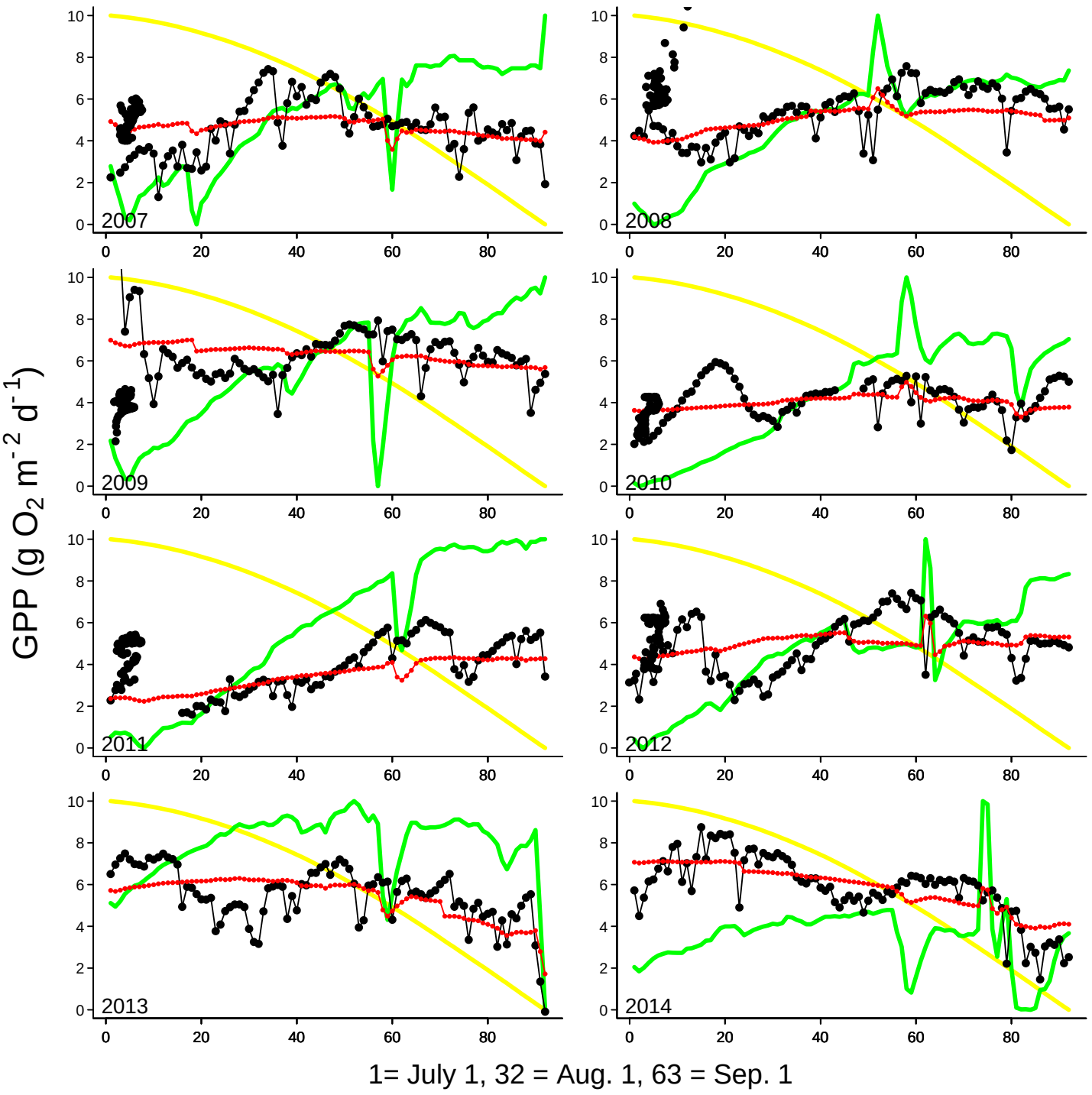

Figure D 4. Modeled GPP for Turwar (red line) with measured GPP (black line) for each of eight study years during July, August, and September. Yellow line is modeled light representing seasonal change in day length and green line represents the fraction of discharge from Iron Gate Dam. Scales for fraction of flow from Iron Gate and light are arbitrary and are used to show trends in these variables.

APPENDIX D: DAILY GRAPHS OF ENVIRONMENTAL DATA AND CALCULATED METABOLISM FOR INDIVIDUAL SITES

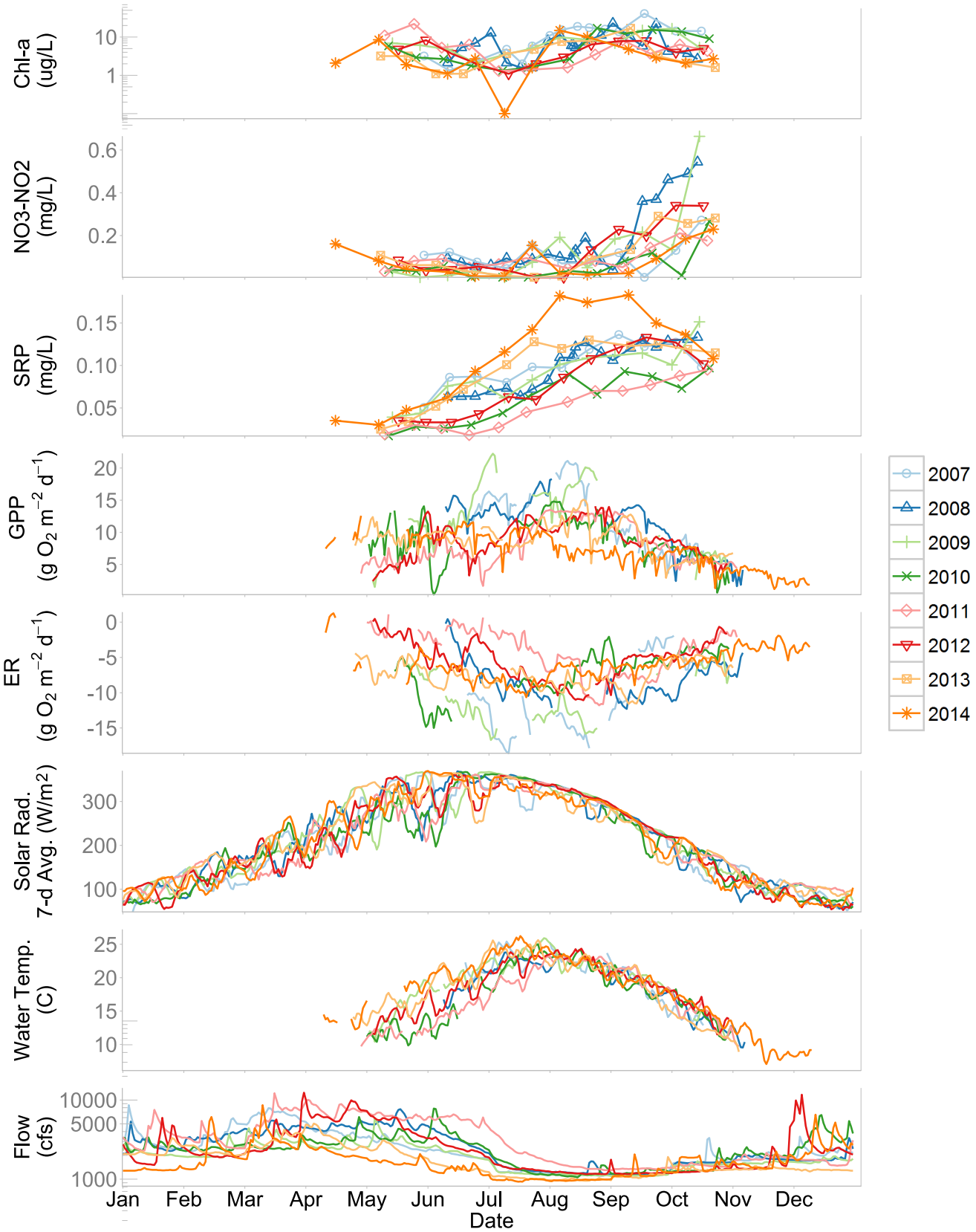

Figure E1. Measured environmental parameters and calculated ER and GPP for Klamath River at Seiad. BGA probes. Solar radiation shown here is a 7-day average of remote-sensed data from the North American Land Data Assimilation System (NLDAS, Xia et al. 2012) and was not used in analysis.

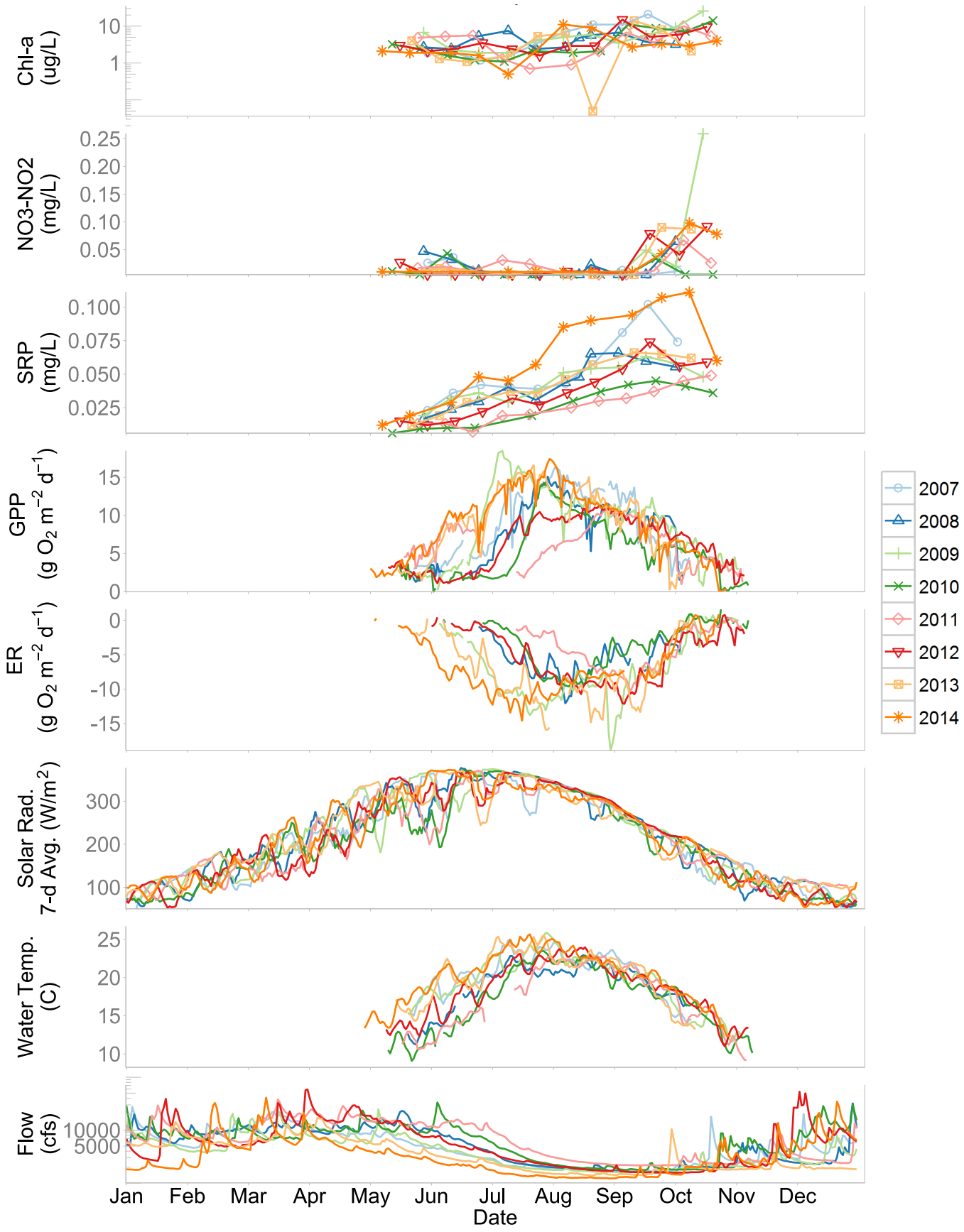

Figure E2. Measured environmental parameters and calculated ER and GPP for Klamath River at Weitchpec. Solar radiation shown here is a 7-day average of remote-sensed data from the North American Land Data Assimilation System (NLDAS, Xia et al. 2012) and was not used in analysis.

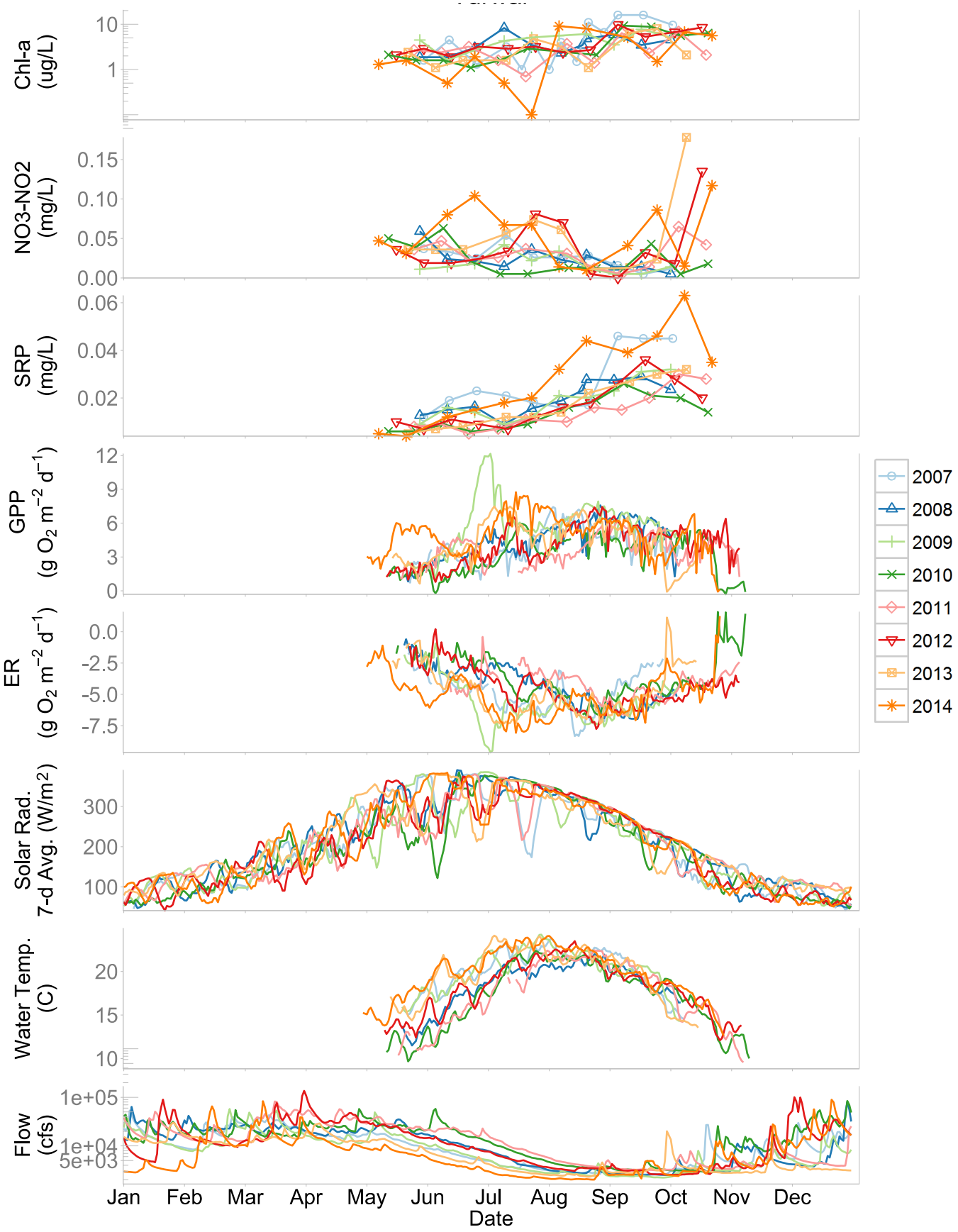

Figure E3. Measured environmental parameters and calculated ER and GPP for Klamath River at Turwar. Solar radiation shown here is a 7-day average of remote-sensed data from the North American Land Data Assimilation System (NLDAS, Xia et al. 2012) and was not used in analysis.